

Brain-Conditional Multimodal Synthesis: A Survey and Taxonomy

Weijian Mai¹, Jian Zhang¹, Pengfei Fang², Zhijun Zhang^{1*}

¹South China University of Technology

²Southeast University

auzjzhang@scut.edu.cn *

Abstract

In the era of Artificial Intelligence Generated Content (AIGC), conditional multimodal synthesis technologies (e.g., text-to-image, text-to-video, text-to-audio, etc) are gradually reshaping the natural content in the real world. The key to multimodal synthesis technology is to establish the mapping relationship between different modalities. Brain signals, serving as potential reflections of how the brain interprets external information, exhibit a distinctive One-to-Many correspondence with various external modalities. This correspondence makes brain signals emerge as a promising guiding condition for multimodal content synthesis. Brain-conditional multimodal synthesis refers to decoding brain signals back to perceptual experience, which is crucial for developing practical brain-computer interface systems and unraveling complex mechanisms underlying how the brain perceives and comprehends external stimuli. This survey comprehensively examines the emerging field of AIGC-based **Brain-conditional Multimodal Synthesis**, termed **AIGC-Brain**, to delineate the current landscape and future directions. To begin, related brain neuroimaging datasets, functional brain regions, and mainstream generative models are introduced as the foundation of AIGC-Brain decoding and analysis. Next, we provide a comprehensive taxonomy for AIGC-Brain decoding models and present task-specific representative work and detailed implementation strategies to facilitate comparison and in-depth analysis. Quality assessments are then introduced for both qualitative and quantitative evaluation. Finally, this survey explores insights gained, providing current challenges and outlining prospects of AIGC-Brain. Being the inaugural survey in this domain, this paper paves the way for the progress of AIGC-Brain research, offering a foundational overview to guide future work. A webpage associated with this survey is available at: <https://github.com/MichaelMaiiii/AIGC-Brain>.

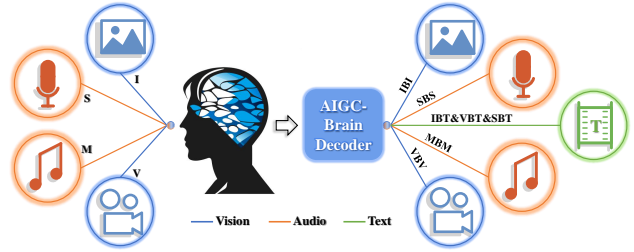


Figure 1. Brain-Conditional Multimodal Synthesis via AIGC-Brain Decoder. Sensory stimuli comprising visual stimuli (Image (I), Video (V)) and audio stimuli (Music (M), Speech/Sound (S)) from the external world are first encoded to non-invasive brain signals (EEG, fMRI, or MEG) and then decoded back to perceptual experience via the AIGC-Brain decoder. This survey focuses on passive brain-conditional multimodal synthesis tasks including Image-Brain-Image (IBI), Video-Brain-Video (VBV), Sound-Brain-Sound (SBS), Music-Brain-Music (MBM), Image-Brain-Text (IBT), Video-Brain-Text (VBT), and Speech-Brain-Text (SBT), where IBI refers to image synthesis tasks conditioned on brain signals evoked by image stimuli.

1. Introduction

Understanding complex mechanisms by which the brain perceives the world is crucial for unraveling the mysteries of human perception [37, 57]. Sensory information is transformed into neural signals and transmitted through the nervous system to various brain regions. The correlation between external stimuli and brain signals provides valuable insights into the neural processes underlying perception [53, 107, 115]. Perception refers to the process by which individuals receive, organize, and interpret sensory stimuli to make sense of the external world. It is not merely the passive reception of sensory inputs; rather, it involves complex cognitive processes that contribute to shaping subjective experience. Hence, decoding brain signals back to perception (e.g., corresponding vision, audio, and descriptive semantic text) holds significance in unraveling the complex mechanisms underlying perception. Moreover, brain perception decoding contributes to developing prac-

*Corresponding author

tical Brain-Computer Interface (BCI) systems. This technological advancement can potentially enhance communication between the brain and external devices, paving the way for novel applications in neuroprosthetics [100, 121], virtual/augmented reality [142, 187], and assistive [24, 28] technologies.

Neuroimaging technologies (e.g., functional Magnetic Resonance Imaging (fMRI), Electroencephalography (EEG), and Magnetoencephalography (MEG)) offer a window into the intricate neural activity associated with perception experiences [32, 33, 68]. Specifically, fMRI captures changes in blood flow with high spatial resolution, making it proficient in localizing brain activity but having limited temporal resolution. EEG records electrical activity on the scalp, providing excellent temporal resolution and sensitivity to neural processes but lacking spatial precision. MEG measures magnetic fields generated by neural activity, offering a balanced combination of spatial and temporal resolution. Neuroimaging data lays the foundation for brain decoding that facilitates the exploration of functionalities and interrelations of various brain regions, shedding light on the operational mechanisms by which the brain perceives and comprehends the external world [52, 135].

Generative models have evolved from deterministic Autoencoders (AEs) [89] to probabilistic models like Variational Autoencoders (VAEs) [87], Autoregressive Models, Generative Adversarial Networks (GANs) [59], and the current hottest Diffusion Models (DMs) [69, 158, 160]. Each development phase represents a significant advancement, incorporating probabilistic aspects, sequential dependencies, adversarial training, and iterative denoising processes, showcasing the continuous innovation in generative modeling. These methods have succeeded in various domains, including image, video, text, and audio synthesis. Conditional generative models extend the concept by introducing conditional information into the generation process, rather than just generating samples randomly from the data distribution [40, 148, 161]. Specifically, image-to-image translation [75] and style transfer [175] within the image modality are based on conditional generative models. Moving further, conditional multimodal generative models integrate information from multiple modalities, including one-to-one synthesis (e.g., text-to-image [146], text-to-video [10], text-to-audio [104], and image-to-text [98], audio-to-video [79]), one-to-any synthesis (e.g., text-to-image&video [189]), any-to-one synthesis (e.g., text&image-to-video [88]), and a unified model for any-to-any synthesis (e.g., text&image-to-video&speech [58, 108]).

The key to multimodal synthesis technology is to establish the mapping relationship between different modalities. Brain signals, serving as potential reflections of how the brain interprets external information, exhibit a distinctive One-to-Many correspondence with various external modal-

ities. This correspondence makes brain signals emerge as a promising guiding condition for multimodal content synthesis [25, 102, 166]. This survey comprehensively examines the emerging field of AIGC-based brain-conditional multimodal synthesis, termed AIGC-Brain, to delineate the current landscape and future direction for further work. Fig. 1 illustrates the pipeline of brain-conditional multimodal synthesis via the AIGC-Brain decoder. Sensory stimuli comprising visual stimuli (i.e., image (I) and video (V)) and audio stimuli (i.e., sound (S), speech (S), and music (M)) from the external world are first encoded to non-invasive brain signals (EEG, fMRI, or MEG) and then decoded back to perceptual experience via the AIGC-Brain decoder. Note that this survey focuses on passive brain decoding tasks where brain signals are evoked from sensory stimuli. So far, various AIGC-Brain decoding tasks have been explored, including Image-Brain-Image (IBI), Video-Brain-Video (VBV), Sound-Brain-Sound (SBS), Music-Brain-Music (MBM), Image-Brain-Text (IBT), Video-Brain-Text (VBT), and Speech-Brain-Text (SBT). Specifically, IBI refers to image synthesis tasks conditioned on brain signals evoked by image stimuli, VBV refers to video synthesis tasks conditioned on brain signals evoked by video stimuli, and so on. AIGC-Brain refers to decoding brain signals back to perception information (e.g., corresponding vision, audio, and semantic text) that contributes to developing practical BCI systems and unraveling how the brain process and understand the external world.

This survey delves into various aspects of AIGC-Brain, concentrating on *passive synthesis tasks* from non-invasive brain signals evoked by sensory stimuli while other AIGC-Brain tasks such as *active synthesis tasks* and *invasive synthesis tasks* are introduced briefly. Note that this survey concentrates on generative tasks, excluding other research areas like retrieval [194], modality matching [36], and classification [45, 131], as they are beyond the scope of this paper. This manuscript contributes significantly to the field in the following aspects:

- **Foundations:** We meticulously summarize related brain neuroimaging datasets, functional brain regions, and mainstream generative models as the foundation of AIGC-Brain decoding and analysis.
- **Methodology Taxonomy:** We systematically categorize AIGC-Brain decoding models based on shared characteristics in their implementation architectures, emphasizing workflows, intrinsic mapping relations, strengths, and weaknesses of each type of method. This methodology taxonomy serves to delineate the current methodological landscape of AIGC-Brain.
- **Task-specific Implementation:** This survey presents detailed implementation strategies for various AIGC-Brain tasks, showcasing representative work and

pipelines, to facilitate comparison and in-depth analysis of technological trends, task-specific characteristics, and preferences.

- **Quality Assessment:** This survey provides an overview of task-specific quality assessments in AIGC-Brain to facilitate the evaluation of synthesis results qualitatively and quantitatively.
- **Comprehensive Insights:** This work concludes with a concise summary of current challenges in AIGC-Brain and provides insightful perspectives for future research directions.

The remainder of this survey is organized as follows. Section 2 and Section 3 provides a comprehensive overview and description of brain neuroimaging datasets and related functional brain regions in AIGC-Brain, respectively. Section 4 introduces mainstream generative models as the methodology foundation of AIGC-Brain. Section 5 provides a comprehensive methodology taxonomy for AIGC-Brain decoding models and Section 6 presents task-specific representative work and detailed implementation strategies. Section 7 reviews task-specific quality assessment with both qualitative and quantitative metrics. In Section 8, we conclude this survey and discuss the main challenges and prospects for AIGC-Brain.

2. Neuroimaging Datasets

Neuroimaging data (e.g., fMRI, EEG, MEG) lays the foundation for brain decoding research that facilitates the exploration of functionalities and interrelations of various brain regions, shedding light on the operational mechanisms by which the brain perceives and comprehends the external world [52, 135]. Constructing neuroimaging datasets involves costly equipment, technical challenges, as well as ethical and privacy concerns. We greatly appreciate the authors' contributions to existing open-source datasets, as they offer a valuable resource for neuroscience and medical research, thereby enhancing our comprehension of the human brain. In this section, we summarize public neuroimaging datasets in terms of brain responses to visual and auditory stimuli that have been used for AIGC-Brain decoding tasks. As shown in Table 1, neuroimaging datasets are divided according to their stimulus modality. For each dataset, the reference source (Dataset), data type (Type), specific experimental paradigm, fMRI region-of-interest or EEG/MEG channels (ROI/Channel), number of subjects (Sub), and associated AIGC-Brain tasks are presented.

2.1. Image Datasets

While there exist a variety of neuroimaging datasets used for brain-conditional image reconstruction, such as

binary contrast patterns (BCP) [118], 6-9 dataset of hand-written digits [180], BRAINS dataset of handwritten characters [150], we focus on the datasets with a higher level of perceptual complexity of presented stimuli: datasets of faces, grayscale natural images, and natural images.

The Natural Scenes Dataset (NSD¹) [2] is currently the largest fMRI-Image dataset gathered from 8 subjects viewing 73,000 natural scene images from the COCO dataset [103]. Researchers usually focus on four subjects (Sub-1, Sub-2, Sub-5, and Sub-7) who finished all viewing trials. The test images (1,000) remain consistent across all subjects, whereas distinct training images (9,000x8) are adopted. NSD is currently one of the most popular image datasets and has been used for IBI [51, 61, 102, 105, 109, 110, 130, 151, 166, 167, 191] and IBT [18, 51, 110] tasks. The corresponding captions in the COCO dataset can serve as semantic descriptions of images. The Generic Object Decoding (GOD²) dataset [71] is an fMRI dataset gathered from 5 subjects viewing 1,250 natural object images from 200 classes of ImageNet. The training set consists of 1,200 images from 150 classes, while the test set comprises only 50 images from 50 classes. Therefore, brain decoding on GOD involves zero-shot learning of category information, and it may fall short in complex scenes with multiple objects. Furthermore, current GOD-based research generally uses BLIP [99] to generate semantic captions to obtain semantic information about images. GOD is also one of the most popular image datasets and has been used for IBI [6, 20, 25, 49, 50, 54, 105, 113, 114, 116, 120, 129, 136, 145, 152, 163, 198] and IBT [165] tasks. The Deep Image Reconstruction (DIR) dataset [155] has the same natural image dataset as GOD, with 40 artificial shapes, and 10 alphabetical letters added during the testing sessions. The Brain, Object, Landscape Dataset (BOLD) [17] and the grayscale natural Vim-1 dataset [85] are generally accompanied by the GOD dataset to verify the generalization ability of the AIGC-Brain decoder. Similar to GOD, the Object Category Decoding (OCD) dataset [74] is gathered from 5 subjects viewing 2,750 (train/valid/test: 2,250/250/250) natural object images from 5 classes of ImageNet. However, it is currently only used for IBT tasks [73, 200]. The Faces dataset [181] is currently the only fMRI dataset focused on face image reconstruction. The EEG Visual Object Analysis dataset (EEG-VOA³) [162] is collected using EEG equipment with 128 channels placed following the international 10–10 system. Similar to GOD, image stimuli in EEG-VOA are from 40 classes of ImageNet, but it only uses a random 8 (train):1 (valid):1 (test) ratio to split the dataset. EEG-VOA is the most popular EEG dataset that has been used for IBI

¹<https://naturalscenesdataset.org>

²<https://github.com/KamitaniLab/GenericObjectDecoding>

³https://github.com/perceivelab/eeeg_visual_classification

Table 1. Neuroimaging Datasets for AIGC-Brain Decoding Tasks.

Modality	Dataset	Type	Experimental Paradigm	ROI / Channel	Sub	AIGC-Brain Task
Image	NSD [2]	fMRI	Viewing 73,000 (72,000/1,000) natural scene images from COCO.	V1, V2, V3, V4, LOC, FFA, PPA	8	IBI [51, 61, 105, 109, 110, 130, 151, 166, 167] IBT [18, 51, 110]
	GOD [71]	fMRI	Viewing 1,250 (1,200/50) natural images from 200-class of ImageNet.	V1, V2, V3, V4, LOC, FFA, PPA	5	IBI [6, 20, 25, 49, 50, 54, 105, 114, 116, 120, 129, 136, 145, 152, 163, 198] IBT [165]
	BOLD [17]	fMRI	Viewing 4,916 distinct scene images from SUN, COCO, and ImageNet.	PPA, RSC, OPA, EVC	4	IBI [25, 136, 163, 198]
	DIR [155]	fMRI	Viewing (or imaging) natural images (Same as GOD), artificial shapes (0/40), and alphabetical letters (0/10).	V1, V2, V3, V4, LOC, FFA, PPA	3	IBI [154, 155]
	Vim-1 [85]	fMRI	Viewing 1,870 (1,750/120) grayscale natural images.	V1, V2, V3, V4, LO	2	IBI [6, 54, 137, 152]
	Faces [181]	fMRI	Viewing 108 (88/20) face images from CelebA.	N/A	4	IBI [181]
	OCD [74]	fMRI	Viewing 2,750 (2,250/250/250) natural images from 5-class of ImageNet.	V1, V2, V3, LVC, HVC, VC	5	IBT [73, 200]
	EEG-VOA [162]	EEG	Viewing 2,000 (1,600/200/200) natural images from 40-class of ImageNet.	128 EEG Channels	6	IBI [4, 80, 84, 86, 94, 132, 199]
	MEG-Things [66]	MEG	Viewing 22,448 object images from 1,854-class from the THINGS database	272 MEG Channels	4	IBI [8]
Video	DNV [188]	fMRI	Viewing 972 (374/598) natural color video clips from VideoBlocks and Youtube.	V1, V2, V3, V4, LO, MT, FFA, PPA, LIP, TPJ, PEF, FEF	3	VBV [26, 63, 93, 183, 188]
	VER [126]	fMRI	Viewing 12,600 (7,200/5,400) color natural clips from the Apple Quick-Time HD gallery and YouTube.	V1, V2, V3, V3A, V3B	3	IBT [111, 112]
Video & Speech	STNS [153]	fMRI	Viewing and listening videos from 30 episodes of BBC's Doctor Who.	V1, V2, V3, MT, AC, FFA, LOC, OFA	1	VBV [96]
	CLSR [170]	fMRI	Viewing silent video clips from animated films. & Listening 82 stories from The Moth Radio Hour and Modern Love.	AC, Broca, sPMv	3	VBT & SBT [170]
Sound & Speech	BSR [134]	fMRI	Listening 1,250 (1,200/50) sound clips from VGGSound test dataset.	A1, LBelt, Pbelt, A4, A5	5	SBS [134]
	Narratives [124]	fMRI	Listening 27 diverse naturalistic spoken stories.	A1, Mbelt, LBelt, Pbelt, RI	345	SBT [190]
	ETCAS [62]	EEG	Listening continuous speech audio from the TIMIT dataset.	24 EEG Channels	50	SBS [62]
Music	MusicGenre [123]	fMRI	Listening 540 (480/60) music pieces from 10 music genres.	N/A	5	MBM [39]
	MusicAffect [35]	fMRI&EEG	Listening Synthetic music and Classical music clips.	N/A & 31 EEG Channels	21	MBM [34]

¹ Public Large Dataset: COCO [103], ImageNet [38], SUN [192], CelebA [106], Things [67], VGGSound [19], TIMIT-<https://catalog.ldc.upenn.edu/docs/LDC93S1/TIMIT.html>

² Website: VideoBlocks-<https://www.videoblocks.com>, Youtu-<https://www.youtube.com>, Apple Quick-Time HD Gallery-<http://trailers.apple.com>

tasks [4, 80, 84, 86, 94, 132, 199]. The MEG-Things⁴ [66] dataset is collected using MEG equipment with 272 MEG channels, while 4 subjects viewed 22,448 unique object images from 1,854 classes in the THINGS [67] database.

⁴<https://things-initiative.org/>

2.2. Video Datasets

The Dynamic Natural Vision (DNV) dataset [188] is collected from 3 subjects viewing natural color video clips. DNV is currently the most popular fMRI-Video dataset for VBV tasks [26, 63, 93, 183, 188]. The Visual Experience Reconstruction (VER) dataset [126] only involves ROIs of

control. The Temporoparietal Junction (TPJ) is involved in various functions, including social cognition, perspective-taking, and attention.

In summary, EVC regions (V1, V2, V3, V4, MT, OFA) primarily handle basic visual processing, while HVC regions (LOC, FFA, PPA, OPA, RSC, LIP, TPJ) are responsible for more advanced visual processing tasks (i.e., face recognition, scene perception, and social cognition). EVC is primarily located in the occipital (O) lobe of the brain. As information progresses from EVC to the HVC, the processing of visual information becomes more complex and abstract. As a result, HVC refers to regions situated at higher levels extending into the temporal (T) and parietal (P) lobes (Fig.2).

3.2. Auditory Cortex

The auditory cortex (AC) is a specific brain region responsible for processing auditory information, including the perception of sound, speech, music, and other auditory stimuli. It is typically located in the temporal (T) lobe (Fig.2). The early auditory cortex (EAC) [119], including A1 (Primary Auditory Cortex), A4, and A5, focuses on fundamental auditory processing, such as pitch and frequency. In contrast, the higher auditory cortex (HAC) [11], comprising the Lateral Belt (LBelt), Posterior Belt (PBelt), Medial Belt (MBelt), and Rostral Intermediate (RI), is involved in more advanced functions like sound localization, integration of complex auditory stimuli, and the comprehensive processing of auditory information in conjunction with other sensory modalities. Together, these distinct areas work in concert to form a sophisticated system for perceiving and interpreting the diverse aspects of auditory stimuli.

3.3. Language Cortex

The language cortex, which is typically located in the Frontal (F) lobe, refers to brain regions that are involved in language processing. It includes various regions responsible for both understanding and producing spoken and written language. Language processing is a complex and distributed function, and it engages several brain areas working in concert. The Broca’s Area (Broca) plays a critical role in language production and speech [122]. It is associated with the ability to form grammatically correct sentences, coordinate the muscles necessary for speech (e.g., lips, tongue, and vocal cords), and generate fluent, coherent language. The Superior Ventral Premotor Speech Area (sPMv) is primarily involved in the motor planning and control of speech production [173]. sPMv is crucial for coordinating the movements of the articulatory muscles, allowing us to produce the precise sounds and phonemes required for spoken language.

4. Generative Models

AIGC-Brain aims to synthesize multimodal content conditioned on brain signals, as shown in Fig.1. The AIGC-Brain decoder is structured with two key elements: the modality matching network and the AIGC decoder. The modality matching network is commonly constructed using linear regressions or simple neural networks. The AIGC decoder typically employs deep generative models including Diffusion Models (DMs), Generative Adversarial Networks (GANs), Variational Autoencoders (VAEs), Convolutional Autoencoders (CAEs), and Autoregressive Models. This section will briefly introduce generative models that have been utilized for AIGC-Brain decoding.

4.1. Diffusion Models

Diffusion Models (DMs) [69] are a class of probabilistic generative models that leverage iterative denoising to transform a sampled variable from Gaussian noise into a sample adhering to the learned data distribution. The forward diffusion process gradually introduces Gaussian noise to the initial input x_0 at each time point, defined as $x_t = \sqrt{\alpha_t}x_0 + \sqrt{1 - \alpha_t}\epsilon_t$. A neural network, termed the denoising U-Net [147], is trained to perform the reverse diffusion process, predicting and removing noise from the noisy input to recover the original variables. The loss function for this process is expressed as:

$$L_{DM} = E_{x_0, \epsilon \sim \mathcal{N}(0,1), t} [||\epsilon - \epsilon_\theta(x_t, t)||^2]$$

where α controls the noise addition, ϵ represents true Gaussian noise, $\epsilon_\theta(\cdot)$ is the neural network predicting the noise, and $t \in \{1, 2, \dots, T\}$ denotes the time step. Specifically, Guided Diffusion (GD) [41] is an instance of a diffusion model that incorporates classifier guidance for image synthesis.

Pixel space DMs come with significant computational costs. Latent Diffusion Models (LDMs), also termed Stable Diffusion (SD) [146], overcome this challenge by compressing the input with an autoencoder $E(\cdot)$ trained on a large-scale image dataset to learn a compressed latent representation z_0 from image x_0 ($z_0 = E(x_0)$). The forward diffusion process in LDM is denoted as $z_t = \sqrt{\alpha_t}z_0 + \sqrt{1 - \alpha_t}\epsilon_t$. The reverse diffusion process introduces additional conditions in a latent space, with an objective function defined as:

$$L_{LDM} = E_{z_0, c, \epsilon \sim \mathcal{N}(0,1), t} [||\epsilon - \epsilon(z_t, t, \tau_\theta(c))||^2]$$

where $\tau_\theta(c)$ is the conditioning input for U-Net. The innovative aspect of LDM lies in its ability to guide the inverse diffusion process using various conditions (e.g., labels, captions, images, and semantic maps). Conditioning

is achieved by integrating conditions $\tau_\theta(c)$ within the cross-attention block of the denoising U-Net model. The denoised latent variable resulting from the reverse diffusion is then passed through the pretrained decoder $D(\cdot)$ to generate a high-quality image.

ControlNet [201] serves as an extra control neural network working with large pretrained text-to-image diffusion models (i.e., Stable Diffusion). Besides text conditions, additional spatial conditions (e.g., human pose, canny edge, and depth map) can be incorporated into diffusion models to further control image generation. Moreover, Versatile Diffusion (VD) [193] stands out as a multi-flow multimodal latent diffusion model with the capacity to generate diverse outputs, such as images and text. The guidance for this versatility comes from CLIP [138] features derived from images, text, or combinations of both. VD serves as an advanced and adaptable model for generating diverse outputs in the context of image and text synthesis.

4.2. Generative Adversarial Networks

Generative Adversarial Networks (GANs) [59] constitute a revolutionary approach to generative modeling. The central idea involves training a generator and discriminator simultaneously through adversarial training. The generator aims to produce synthetic data that is indistinguishable from real data, while the discriminator works to differentiate between real and generated samples. This adversarial game is formulated with the following objective function:

$$\min_G \max_D V(D, G) = \mathbb{E}_{x \sim p_{\text{data}}(x)} [\log D(x)] + \mathbb{E}_{z \sim p_z(z)} [\log(1 - D(G(z)))]$$

In the realm of image generation, GANs have achieved unparalleled success, generating high-quality, diverse images with realistic details. Their applications extend to various domains, including video synthesis (e.g., Vid2Vid [185], MoCoGAN [174], and TGAN [149]), audio generation (e.g., WaveGAN [43] and GAN-TTS [9]), and image synthesis (e.g., DCGAN [139], StyleGAN [82], StyleGAN2 [83], BigGAN [137], PGGAN [81]). Conditional GANs (cGANs) such as InfoGAN [22], ICGAN [15], CycleGAN [204], and Pix2Pix [76] are an extension of the traditional GANs that incorporate additional conditional information during the training and generation processes. GANs' ability to capture intricate patterns and produce compelling, life-like content positions them at the forefront of generative modeling. While GANs offer remarkable advantages, such as the production of realistic samples and their versatility across domains, challenges persist, including training instability, convergence issues, and mode collapse.

4.3. Variational Autoencoders

Variational Autoencoders (VAEs) [87] represents a prominent paradigm in generative modeling, combining variational inference and autoencoder architecture. The fundamental principle involves encoding input data x into a probability distribution in the latent space, facilitating stochastic sampling and decoding for accurate reconstruction. The VAE objective function is defined as:

$$\mathcal{L}_{\text{VAE}} = \mathbb{E}_{q(z|x)} [\log p(x|z)] - \text{KL}(q(z|x)||p(z))$$

where the first term represents the reconstruction loss, and the second term is the Kullback-Leibler divergence between the distribution of latent variables given the data ($q(z|x)$) and a prior distribution ($p(z)$).

As variants of VAEs, VQ-VAE [178] introduces vector quantization to enhance discrete latent variable representations and is further improved by VQ-VAE2 [143]. Conditional VAE (CVAE) [159] incorporates conditional information during the generation process, offering contextual considerations. VAEs excel in learning interpretable latent representations but may generate blurry samples. To address this, VAE-GAN [95] combines VAEs with GANs to enhance sample quality by integrating adversarial training. This hybrid model holds promise in producing refined and diverse samples, overcoming VAE limitations.

4.4. Convolutional Autoencoders

The Convolutional Autoencoder (CAE) [203], operating as a deterministic generative model, leverages convolutional neural networks (CNNs) for both encoding and decoding processes. The encoder utilizes convolutional layers to extract hierarchical features from the input data, transforming it into a latent representation. The decoder, which typically employs deconvolutional layers or transposed convolutions, then reconstructs the input from this latent space. This deterministic architecture finds extensive application in the generation domain, excelling in tasks such as image denoising [127], image compression [27], and image-to-image translation [195].

One notable distinction from probabilistic generative models lies in the deterministic nature of CAE. Unlike probabilistic models that provide a distribution of possible outputs, the deterministic model ensures a single, consistent reconstruction for a given input. This characteristic makes it computationally efficient and suitable for applications where deterministic outputs are preferred. While CAE exhibits advantages in capturing complex patterns and spatial dependencies, it may face challenges such as overfitting training data, limited semantic expressiveness, and poor diversity compared to its probabilistic counterparts.

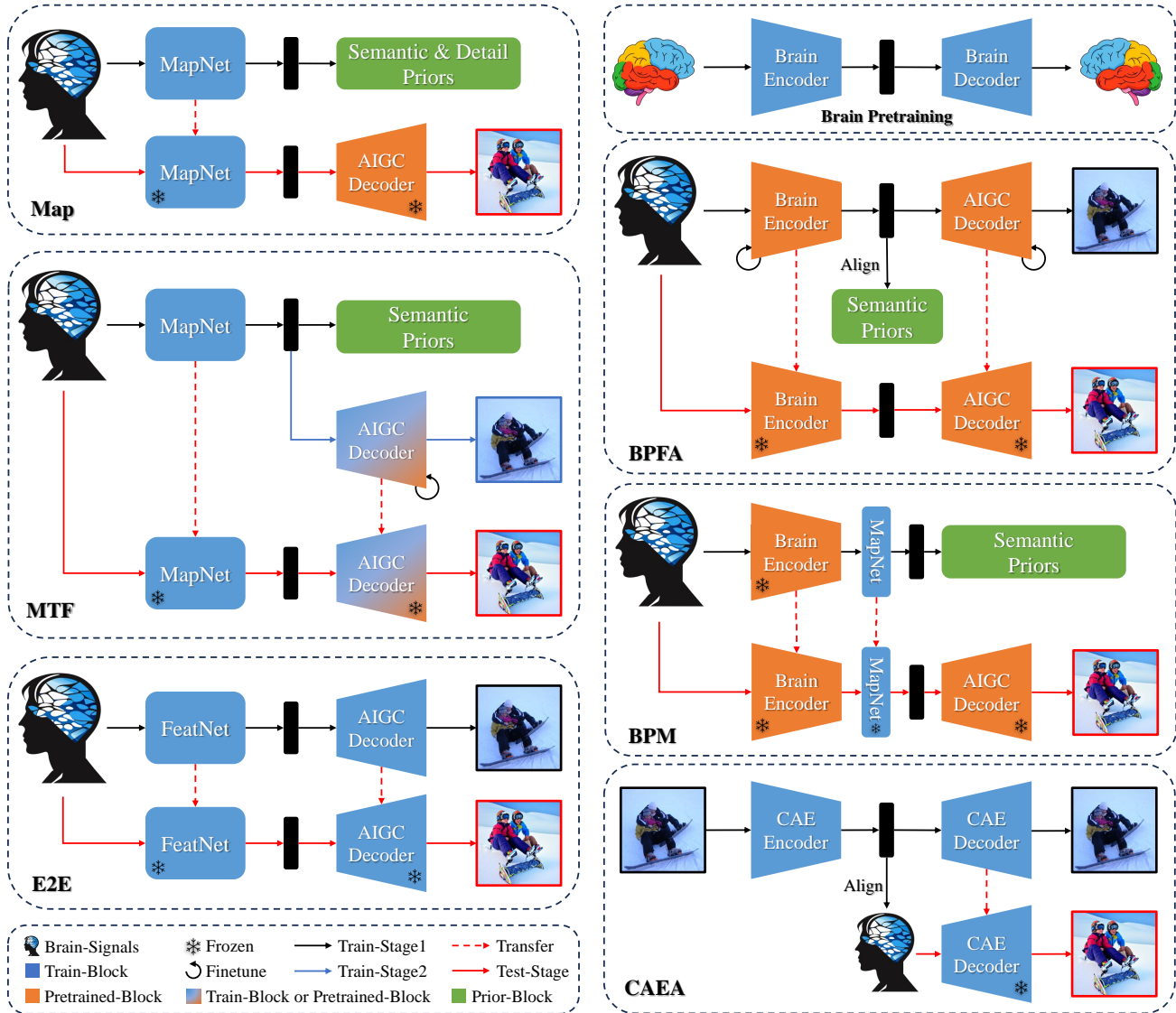


Figure 3. Different types of methods for AIGC-Brain tasks. Map: Mapping; MTF: Map&Train&Finetune; E2E: End-to-End; BPM: Brain-Pretrain⤅ BPF: Brain-Pretrain&Finetune&Align; AEA: Auto-Encoder&Align. Brain pretraining on large-scale neuroimaging datasets (e.g., HCP [179] and MOABB [78]) is the first stage of BPF and BPM methods.

4.5. Autoregressive Models

Autoregressive models have evolved substantially, progressing from Gate Recurrent Unit (GRU) [29] and Long-Short Term Memory (LSTM) [70] architectures to the transformative Transformer [182] model. Originally designed to address sequential dependencies, GRU and LSTM introduced gating mechanisms in recurrent neural networks (RNNs). The Transformer architecture revolutionized sequence modeling by leveraging self-attention mechanisms, allowing for parallelization and capturing long-range dependencies efficiently.

Across diverse domains, autoregressive models have demonstrated remarkable efficacy. In natural language processing, particularly text-related tasks, models like GPT (Generative Pre-trained Transformer) series (i.e., GPT [140], GPT-2 [141], GPT-3 [12], GPT-4 [13]) showcase state-of-the-art language understanding and generation capabilities. Adapting to image generation, autoregressive structures, exemplified by PixelRNN [177], PixelCNN [176], and transformer-based models (e.g., Taming [48], iGPT [21], CogView [42], and ImageBart [47]), predict pixel values or tokens sequentially. In audio processing, autoregressive models such as WaveNet [128] excel in gen-

Table 2. Different Method Types and Related Information for AIGC-Brain Tasks.

Method Type	Mapping Relation	Description	Strength	Weakness	References
Map	Brain-Prior	Map brain signals to semantic or detail priors of the pre-trained AIGC decoder.	Easy training Flexible implementation High fidelity	Bias superposition	IBI: [8, 20, 49–51, 61, 94, 102, 105, 109, 110, 113, 114, 116, 120, 129, 130, 137, 151, 152, 155, 166, 167, 181, 191] VBV: [63] SBS: [134] MBM: [39] IBT: [18, 110–112, 165] VBT&SBT: [170]
BPM	Brain-Prior	Pretrain on brain signals and then map to semantic priors of the pretrained AIGC decoder.	High semantic fidelity	Bias superposition Hard pretraining	IBI: [136] SBT: [190]
BPFA	Brain-Prior-Stimuli	Pretrain on brain signals and then finetune the pretrained AIGC decoder with/without semantic prior alignment.	High semantic fidelity	Hard pretraining Hard finetuning	IBI: [4,25,163,198] VBV: [26]
MTF	Brain-Prior-Stimuli	Map brain signals to semantic priors, then train from scratch or finetune the AIGC decoder.	High semantic fidelity	Hard training Hard finetuning	IBI: [80, 84, 86, 132, 145, 199] IBT: [73]
E2E	Brain-Stimuli	Map brain signals directly to sensory stimuli.	Simplicity Real-time application	Poor interpretability Low semantic	IBI: [154] VBV: [96, 183] IBT: [200] MBM: [34]
CAEA	Brain-Stimuli	Map brain signals directly to sensory stimuli in a deterministic manner.	High detail fidelity	Low realistic Low semantic	IBI: [6, 54, 55] VBV: [93, 188]

erating high-fidelity audio waveforms.

Autoregressive models excel at capturing sequential dependencies and possess the ability to generate diverse and realistic outputs, notably in text, image, and audio generation. However, challenges persist, with sequential processing impacting training and inference speed. Additionally, capturing extensive dependencies and mitigating vanishing or exploding gradients pose ongoing challenges.

5. AIGC-Brain Methodology Taxonomy

Currently, the advancement in AIGC-Brain is constrained by challenges such as the inherent noise and variability in brain signals, the limited availability of brain-stimulus data pairs, the modality matching between brain and external modalities, and the integration of multimodal generative models. In this survey, we summarize the recent AIGC-Brain decoding models and categorize them into six types of methods according to their architecture: Map, Brain-Pretrain&Map (BPM), Brain-Pretrain&Finetune&Align (BPFA), Map&Train&Finetune (MTF), End-to-End (E2E), and Convolutional-Autoencoder&Align (CAEA). Table 2 summarizes the mapping relation, descriptions, strengths, and weaknesses of each type of method, along with the corresponding AIGC-Brain tasks and models based on these methods. Furthermore, since all methods have been applied to the IBI task, we draw the framework diagram of

each method for comparison by taking the IBI task as an example, as shown in Fig.3. Note that the pretrained AIGC decoders are pretrained on mainstream data such as text, images, videos, and audio. Within the brain-pretraining stage, the brain encoder and decoder are pretrained on large-scale neuroimaging datasets, i.e., fMRI-based dataset HCP [179], and EEG-based dataset MOABB [78] used in DreamDiffusion [4].

5.1. Map

The Map method refers to mapping brain signals to low-level detail priors or high-level semantic priors of the pre-trained AIGC decoder (Fig.3-Mapping). The Map method only constructs the brain-prior connection between brain signals and prior knowledge, which leads to a problem that biases generated in the mapping space tend to stack into the generation space leading to semantic ambiguity (Table 2). However, in this AIGC era, the Map method is currently the most popular method that covers all AIGC-Brain tasks due to its characteristics of easy training, flexible implementation, and high generation quality. In the Map method, the purpose of the mapping network is to map brain signals into prior spaces of the pretrained AIGC decoder, that is, to establish the connection between brain signals and priors (i.e., detail and/or semantic priors). Upon this, specific modality content can be synthesized by the pretrained AIGC decoder. Overall, the research cores of the Map method lie in two as-

pects as follows: i) how to choose and integrate powerful pretrained AIGC decoders to improve multimodal synthesis capabilities, and ii) how to design mapping networks to reproduce more accurate prior information from brain signals.

5.2. Brain-Pretrain&Finetune&Align

The Brain-Pretrain&Finetune&Align (BPFA) method consists of two stages: i) Brain pretraining using large neuroimaging datasets to learn latent features from brain signals, and ii) Finetune the pretrained AIGC decoder using latent features with/without semantic prior alignment (Fig.3-BPFA). When finetuning, BPFA is equivalent to transferring the semantic prior knowledge of the pretrained AIGC decoder (e.g., class priors from the label-to-image decoder) to brain latent features under the objective constraints of sensory stimuli, thus constructing the brain-prior-stimuli connection. BPFA addresses bias superposition in the Map method, but the issue of semantic ambiguity still remains. The problem with BPFM is that both stage-1 pretraining and stage-2 finetuning are relatively difficult to achieve. Therefore, the use of BPFM mainly focuses on a small number of IBI and VBV tasks (Tabel 2).

5.3. Brain-Pretrain&Map

The Brain-Pretrain&Map (BPM) method follows the idea of mapping but uses brain latent features instead of brain signals. BPM first performs brain pretraining to extract latent features, just as done in stage-1 of BPFA. Next, latent features are mapped to semantic priors of the pretrained AIGC decoder (Fig.3-BPM). It has not been proven that latent features are inherently superior to raw brain signals, as the performance of downstream tasks is influenced by the nature of pretraining tasks. Furthermore, pretraining on large neuroimaging datasets is a time-consuming and computationally expensive task. As a result, only a few studies and tasks have used the BPM method (Table 2).

5.4. Map&Train&Finetune

The Map&Train&Finetune (MTF) method also establishes a connection between the brain, prior, and stimuli, but in a different way. In the first stage, MTF maps brain signals to semantic priors, as in the Map method. In the second stage, MTF prefers to train the AIGC decoder from scratch or finetune the pretrained AIGC decoder (Fig.3-MTF). However, training or finetuning deep generative models is challenging due to the scarcity of brain-stimuli pair data and the low signal-to-noise ratio of non-invasive brain signals (Tabel 2). We found that most typical models for EEG-based IBI tasks are dependent on this method, except the state-of-the-art methods like DreamDiffusion [4] and NeuroImagen [94].

5.5. End-to-End

The End-to-End (E2E) method refers to mapping brain signals directly to sensory stimuli by training the AIGC decoder from scratch with/without the feature extractor. E2E establishes the brain-stimuli connection by mapping brain signals directly to sensory stimuli (Fig.3-E2E). It provides a simple architecture suitable for real-time applications. However, the scarcity of data pairs poses a challenge to effectively investigate the semantic information of brain signals, and the "black-box" design of its architecture hinders interpretability (Tabel 2).

5.6. Convolutional-Autoencoder&Align

The Convolutional-Autoencoder&Align (CAEA) method establishes a direct and deterministic connection between brain signals and stimuli by aligning brain signals with the latent features of CAE (Fig.3-CAEA). Currently, CAEA has been applied to visual-related tasks (i.e., IBI and VBV), and modality alignment in CAEA mainly depends on supervised and self-supervised learning [6, 54]. The CAE decoder usually consists of deconvolutional neural networks (DeCNNs) that prioritize generating pixels and outlines of visual stimuli but fall short in semantic and realistic aspects (Tabel 2). Thus, the CAE decoder can function as the mapping network incorporated into the Map method. In this case, reconstructed brain-conditional images from CAEA can serve as image conditions within the Image-to-Image pipeline, offering low-level detail priors for subsequent conditional generative models.

6. AIGC-Brain Tasks&Implementations

In this section, we delve into the intricacies of each AIGC-Brain task, offering a detailed analysis that integrates AIGC-Brain implementation strategies. The recent advancements in AIGC-Brain, spanning various tasks, are succinctly summarized in Table 3. This table systematically organizes each model based on its specific task and dataset, providing details on the employed methods (outlined in Section 5), networks, detail priors, semantic priors, AIGC decoders, and decoder types. Here, the term 'Network' refers to corresponding networks utilized by different methods, that is, the mapping network (MapNet) in Map and MTF methods, the feature network (FeatNet) in the E2E method, the CAE encoder in the CAEA method, and the brain encoder with the mapping/alignment network (represented as encoder&network) in BPM and BPFA methods, respectively.

For a comprehensive overview, we primarily focus on introducing pertinent work associated with representative datasets for each task in Table 3. Unmentioned datasets and their related work are cataloged in the 'task' column of Table 1, and implementation details can be found in their re-

Table 3. AIGC-Brain Decoding Models for AIGC-Brain Tasks.

AIGC Task	Dataset	Model	Method	Network	Detail	Semantic	Decoder	Type		
IBI	NSD	BrainSCN [61]	Map	SCN	Noise Vector	Instance Features (SwAV)	ICGAN [15]	GAN		
		MindReader [102]	Map	CNN	-	CLIP-Text&Image	StyleGAN2 [83]	GAN		
		BrainSD [166]	Map	Ridge	Pixel	-	CLIP-Text	SD [146]	Diffusion	
		BrainSD-TGD [167]	Map	Ridge	Pixel&Depth	-	CLIP-Text	SD [146]	Diffusion	
		BrainCLIP [105]	Map	VAE	Pixel (Retrieval)	-	CLIP-Text&Image	GD [41]	Diffusion	
		BrainDiffuser [130]	Map	Ridge	Pixel	-	CLIP-Text&Image	VD [193]	Diffusion	
		MindDiffuser [109]	Map	Ridge	Pixel	-	CLIP-Text&Image	SD [146]	Diffusion	
		UniBrain [110]	Map	Ridge	Pixel	-	CLIP-Text&Image	VD [193]	Diffusion	
		MindEye [151]	Map	MLP	Pixel	-	CLIP-Image	VD [193]	Diffusion	
	Dream [191]	Map	CNN&MLP	Color&Depth	-	CLIP-Text&Image	SD [146]	Diffusion		
	GOD/BLOD	Mind-Vis [25]	BPFA	MAE/-	-	-	fMRI Features	SD [146]	Diffusion	
		CMVDM [198]	BPFA	MAE/-	Silhouette	-	fMRI Features	SD+ControlNet [201]	Diffusion	
		CAD [163]	BPFA	DC-MAE/Attention	-	-	fMRI&Visual	SD [146]	Diffusion	
	GOD	LEA [136]	BPM	MAE/Ridge	-	-	CLIP-Image	MaskGIT [16]	Autoregressive	
		DBDM [113]	Map	MLP	Pixel	-	CLIP-Text&Image	SD [146]	Diffusion	
		SBD [50]	Map	Ridge	-	-	Deep-Visual (ResNet)	SD [146]	Diffusion	
		BrainICG [129]	Map	Ridge	Noise Vector	-	Instance Features (SwAV)	ICGAN [15]	GAN	
		BrainHSG [114]	Map	DNN	Shallow-Visual (ResNet)	-	Deep-Visual (VGG)	GAN	GAN	
		BrainHVAE [116]	Map	FCN	Shallow-Visual (VGG)	-	Deep-Visual (VGG)	VAE	VAE	
		BrainDCG [152]	Map	Ridge	Shallow-Visual (AlexNet)	-	Deep-Visual (AlexNet)	DCGAN [139]	GAN	
		DIR [155]	Map	SLR	Shallow-Visual (VGG)	-	Deep-Visual (VGG)	DGN [125]	GAN	
		BrainSSG [49]	Map	FCN&DNN	Shape	-	Class Features	I2I-GAN [77]	GAN	
		BrainBBG [120]	Map	Ridge	-	-	Latent Vectors	BigBiGAN [44]	GAN	
		SSNIR [6]	CAEA	CNN	-	-	fMRI&Visual	DeCNN	CAE	
		SSNIR-SC [54]	CAEA	CNN	-	-	fMRI&Visual	DeCNN	CAE	
		SSDR [55]	CAEA	CNN	-	-	fMRI&Visual	DeCNN	CAE	
		BrainDVG [145]	MTF	MLP	-	-	Latent Vectors	VAE-GAN	VAE&GAN	
		E-DIR [154]	E2E	-	-	-	fMRI Features	GAN	GAN	
	EEG-VOA	DreamDiffusion [4]	BPFA	MAE/Projection	-	-	EEG&CLIP-Image	SD [146]	Diffusion	
		NeuroImagen [94]	Map	Extractors	Pixel	-	CLIP-Text	SD [146]	Diffusion	
		DM-RE2I [199]	MTF	EVRNet	-	-	Class Features	DDPM	Diffusion	
		NeuroVision [86]	MTF	LSTM+FCN	-	-	Class Features	C-PGGAN	GAN	
		EEG-VGD [80]	MTF	CNN	-	-	Class Features	GAN	GAN	
		EEG-GAN [132]	MTF	LSTM	-	-	Class Features	GAN	GAN	
	Brain2Image [84]	MTF	LSTM	-	-	Class Features	VAE/GAN	VAE/GAN		
	MEG-Things	MEG-BD [8]	Map	CNN	Pixel	-	CLIP-Text&Image	SD [146]	Diffusion	
	VBV	DNV	DNV [188]	CAEA	CNN	-	fMRI Features	DeCNN	CAE	
			SSRNM [93]	CAEA	CNN	-	fMRI&Visual	DeCNN	CAE	
			BrainViVAE [63]	Map	LR	-	-	Latent Vectors	VAE	VAE
			f-CVGAN [183]	E2E	FCN	-	-	fMRI Features	GAN	GAN
		Mind-Video [26]	BPFA	MAE/Contrastive	-	-	fMRI&CLIP	Augmented SD	Diffusion	
	STNS	Brain2Pix [96]	E2E	-	-	-	fMRI Features	GAN	GAN	
SBS	BSR	BSR [134]	Map	Ridge	-	Deep-Sound (DNN)	Audio-Transformer	Autoregressive		
	ETCAS	ETCAS [62]	E2E	-	-	EEG Features	Dual-DualGAN	GAN		
MBM	MusicGenre	Brain2Music [39]	Map	Ridge	w2v-BERT Tokens	MuLan Embedding	MusicLM [1]	Autoregressive		
	MusicAffect	NDMusic [34]	E2E	-	-	fMRI-EEG Features	BiLSTM	Autoregressive		
IBT	NSD	UniBrain [110]	Map	Ridge	Word&Sentence	CLIP-Text&Image	VD [193]	Diffusion		
		BrainCaptioning [51]	Map	Ridge	-	-	CLIP-Image	GIT [184]	Autoregressive	
		DreamCatcher [18]	Map	FCN	-	-	GPT-Embedding	LSTM	Autoregressive	
	OCD	GIC-PTL [73]	MTF	BiGRU	-	-	Deep-Visual (CNN)	GRU	Autoregressive	
		GIC-CT [200]	E2E	CNN	-	-	fMRI Features	Transformer	Autoregressive	
	VER	DSR [112]	Map	FCN	-	-	Deep-Visual (VGG)	FCN	Autoregressive	
GNLD [111]		Map	MLP	-	-	Deep-Visual (VGG)	LSTM	Autoregressive		
SBT	Narratives	UniCoRN [190]	BPM	CAE/Projection	-	BART-Embedding	BART [97]	Autoregressive		
SBT&VBT	CLSR	CLSR [170]	Map	Ridge	-	GPT-Embedding	GPT [140]	Autoregressive		

¹ The term 'Network' refers to corresponding networks utilized by different methods corresponding to Fig.3, that is, the mapping network (MapNet) in Map and MTF methods (separate different detail and semantic mapping networks by '&'), the feature network (FeatNet) in the E2E method, the CAE encoder in the CAEA method, and the brain encoder with mapping/alignment network in BPM and BPFA methods (denoted as 'brain-encoder/network'), respectively.

spective original papers to which we kindly direct the reader for a more in-depth understanding.

6.1. Image-Brain-Image

The Image-brain-Image (IBI) task has garnered significant attention in the current AIGC-Brain domain, with a considerable body of research. In this session, we primarily consolidate the efforts undertaken on the fMRI-Image datasets (NSD and GOD), the EEG-Image dataset (EEG-VOA), and the MEG-Image dataset (MEG-Things).

Image-to-image latent diffusion models (I2I-LDMs), incorporating pixel detail priors and CLIP semantic conditional priors, stand out as the current state-of-the-art models across all representative datasets for the IBI task (NSD: BrainSD, BrainDiffuser, UniBrain, MindEye; GOD: DBDM; EEG-VOA: NeuroImagen; MEG-Things: MEG-BD). The framework of brain-conditional I2I-LDMs based on the Map method is illustrated in Fig.4. Specifically, brain signals evoked by image stimuli are first mapped to pixel priors and CLIP semantic priors. Following this, the pixel priors are decoded into pixel images, serving as the initial guess. The I2I-LDM decoder further involves the forward noise-adding process and CLIP-guided backward denoising processes, ultimately culminating in the production of high-quality images. Note that CLIP semantic priors consist of CLIP-Text and/or CLIP-Image features derived from the pretrained text and image encoders of CLIP [138].

6.1.1 fMRI-Based Models

NSD-Based Upon the NSD dataset, all decoding models leverage the Map method with mapping networks and pretrained AIGC decoders including Diffusion and GAN. Linear regressions (i.e., Ridge regression and sparse linear regression (SLR)) are commonly used as mapping networks between fMRI voxels and prior information. BrainSCN [61] introduces a surface-based convolutional neural network (SCN) to map fMRI voxels to noise vectors and instance features extracted from pretrained SwAV [14], which are then decoded into images by the generator of pretrained ICGAN [15]. In the case of MindReader [102], a typical CNN and StyleGAN2 [83] are employed without incorporating detail priors. Notably, BrainSD pioneers the utilization of Ridge regression and the I2I pipeline with Stable Diffusion (SD) for IBI tasks (Fig.4). Subsequent studies are built upon this foundation, making enhancements such as replacing simple linear regression with non-linear neural networks (e.g., CNN, VAE, multilayer perception (MLP)), incorporating additional details like depth and color, introducing dual conditions from CLIP (CLIP-Text&Image) to enhance semantic fidelity, and using more powerful diffusion models (e.g., Versatile Diffusion (VD) [193], Guided Diffusion (GD) [41]). These changes are easy to implement

as mapping networks are lightweight and work independently. The most important thing is to select an appropriate pretrained AIGC decoder to combine the mapped prior information of each part for image generation.

GOD-Based Upon the GOD dataset, AIGC-Brain decoding models mainly leverage the Map, BPFA, and AEA methods. In terms of the Map method, DBDM is the state-of-the-art model that utilizes brain-conditional I2I-LDMs with a mapping network of MLP, as depicted in Fig.4. BrainICG resembles BrainSCN except for the mapping networks (SCN vs. Ridge). BrainSSG utilizes a fully connected network (FCN) and deep neural network (DNN) to map fMRI voxels to shape detail priors and semantic class features from image labels, respectively. Moreover, brain signals can be mapped to hierarchy visual features extracted from pretrained deep neural networks (e.g., ResNet [65], VGG [156], AlexNet [90]) or latent vectors extracted from pretrained AIGC decoders (e.g., BigBiGAN [44], VAE [87]). Hierarchy visual features encompass detail features from shallow layers (Shallow-Visual) and semantic features from deep layers (Deep-Visual), which can be further decoded into images by pretrained AIGC decoders (e.g., VAE, DCGAN [139], and deep generator network (DGN) [125].

The BPFA method, along with Diffusion decoders, is currently the state-of-the-art method when conducting the IBI task on GOD, BLOD, and the EEG-VOA datasets. As a pioneer work, Mind-Vis employs Masked Autoencoders (MAE) [64] for brain pretraining on the large-scale unlabeled fMRI dataset HCP [179]. MAE enables the model to learn meaningful representations by partially hiding and reconstructing the input data in the pretraining stage. After that, the brain encoder and the attention layer of the pretrained SD model are finetuned to generate brain-conditional images. Mind-Vis [25] open-sources the pretrained weights that enable subsequent work to improve upon them. CVMDM [198] designs an extra brain-to-silhouette decoder for detail priors and combines them with SD using the idea of ControlNet [201] in the finetuning stage, thus improving the generation performance of Mind-Vis. CAD [163] performs brain pretraining on the HCP dataset using Double-Contrastive MAE (DC-MAE) inspired by previous work in visual contrastive learning [23]. DC-MAE helps identify common patterns of brain activity across populations rather than individual variations. Furthermore, CAD designs a cross-attention layer to perform cross-modal alignment between brain and visual information during finetuning. The BPM-based method LEA [136] employs MAE for brain pretraining and adopts Ridge regression to map brain latent features to CLIP-Image semantic priors. Unlike other AIGC-Brain decoders, LEA utilizes the autoregressive-based Masked Generative Image Transformer (MaskGIT) [16] for image generation.

The BPFA method is limited by its characteristics of hard-pretraining and hard-finetuning. A critical constraint is the necessity for proximity between the pretraining and fine-tuning datasets, introducing challenges when dealing with divergent data types (e.g., fMRI vs. EEG) and varying data lengths (e.g., HCP vs. NSD). Consequently, the adoption of this methodology is hindered, with scant utilization observed in the literature. Researchers predominantly rely on pretrained weights sourced from Mind-Vis, trained on the HCP dataset, and apply them to downstream datasets such as GOD and BOLD. These challenges underscore the necessity for more adaptive approaches in pretraining, especially when confronted with the inherent heterogeneity across neuroscientific datasets.

Furthermore, SSNIR, SSNIR-SC, and SSSDR employ the CAEA method with modality alignment using supervised learning (SL) and self-supervised learning (SSL) for IBI tasks. They mainly consist of three stages: i) Image-to-Brain CAE encoder training (SL), ii) Brain-to-Image CAE decoder training (SL), and iii) Image-to-Image CAE decoder training (SSL). However, their generated images tend to be more inclined to low-level details but lack semantics and authenticity. To tackle this problem, generated images from CAEA can serve as image conditions within the Image-to-Image pipeline, offering low-level detail priors for subsequent conditional generative models. Specifically, Dream [191], the Map-based model, adopts SSSDR [55] as the mapping network to map brain signals to color and depth images for detail priors.

6.1.2 EEG-Based Models

The MTF method is mainly used for EEG-based IBI tasks. Unlike fMRI voxels in one dimension, EEG signals are typically two-dimensional data involving time and channels. Therefore, typical mapping networks in MTF are neural networks like LSTM, CNN, GRU, MLP, and FCN. Researchers first establish the relationship between EEG signals and class labels, high-level visual information, or latent vectors via the mapping network. Then, the mapped semantic features are transmitted to the AIGC decoder for finetuning or training from scratch. Specifically, DM-RE2I [199] introduces a well-designed residual network EVRNet for class features and trains a denoising diffusion probabilistic model (DDPM) [69] for image synthesis. NeuroVision [86] combines LSTM and FCN for feature extraction and trains a class-conditional PGGAN (C-PGGAN) for image generation. Recently, based on the BPFA method, DreamDiffusion [4] reaches state-of-the-art performance in EEG-based IBI tasks following the idea of Mind-Vis. DreamDiffusion collects a large-scale unlabeled EEG dataset on the MOABB [78] platform and performs brain pretraining on it using the MAE method. In the finetuning stage, DreamD-

iffusion follows the basic idea of Mind-Vis and employs a projection layer to align brain latent representation with CLIP-Image semantic information. DreamDiffusion employs a similar approach to Mind-Vis in the EEG domain, but its pretraining dataset and weights have not been released so far. Based on the Map method, NeuroImagen employs detail and semantic extractors to map EEG signals to pixel and CLIP-Text priors, which are then decoded by pretrained SD following the image-to-image pipeline (Fig.4).

6.1.3 MEG-Based Models

MEG-BD [8], the sole existing investigation on the MEG-Things dataset, employs the Map methodology that leverages CNN as the mapping network and I2I-LDM as the AIGC-Brain decoder, as illustrated in Fig.4. Diverging from the prevalent usage of fMRI and EEG modalities, MEG uniquely ensures temporal and spatial resolution concurrently. This pioneering work lays the foundation for the exploration of the MEG-based IBI tasks.

6.2. Video-Brain-Video

Video-Brain-Video (VBV) tasks are addressed using Map, BPFA, and E2E decoding methods. BrainViVAE [63] employs linear regression to map brain signals to latent vectors of the pretrained VAE, which are then decoded into videos. f-CVGAN [183] and Brain2Pix [96] utilize end-to-end GAN models that directly connect brain signals to corresponding videos without relying on prior information. SSRNM [93] follows the idea of CAEA-based image-generated models (i.e., SSNIR, SSNIR-SC, and SSSDR) and extends it for VBV tasks. Additionally, Wen et al. [188] employ a simple version of CAEA that relies solely on supervised learning for modality alignment. Building on the BPFA method, Mind-Video [26] extends the work of Mind-Vis in the VBV domain. Mind-Video leverages the pretrained brain encoder from Mind-Vis for brain latent features, aligning them with CLIP-Image and CLIP-Text features using contrastive learning. The video generation process incorporates an augmented stable diffusion model with spatial and temporal attention. During the finetuning stage, adversarial semantic features derived from fMRI act as guidance for video generation. Mind-Video serves as the state-of-the-art model for VBV tasks and its inference process is depicted in Fig.5.

6.3. Sound-Brain-Sound

In the realm of SBS tasks, our investigation has identified two relevant works grounded in the Map and E2E methodologies. ETCAS [62], an end-to-end GAN model tailored for EEG-based SBS tasks, introduces a Dual-DualGAN to directly map EEG signals to speech signals. In particular, BSR [134], adopting the Map method with an autore-

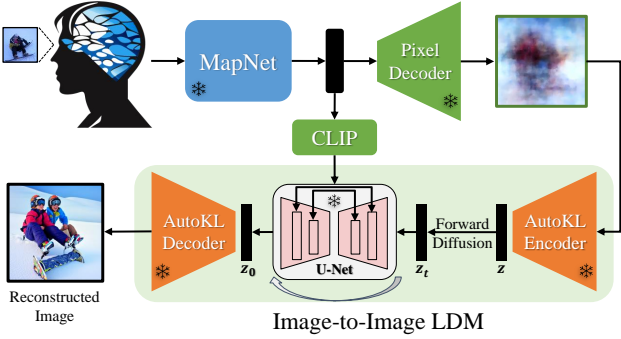


Figure 4. Brain-Conditional I2I-LDMs: State-of-the-art framework for IBI tasks.

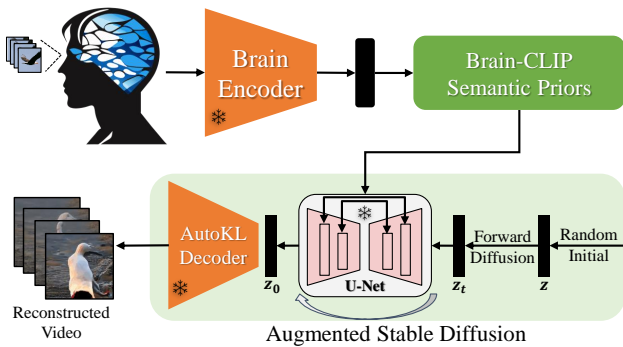


Figure 5. Mind-Video [26]: State-of-the-art model for VBV tasks.

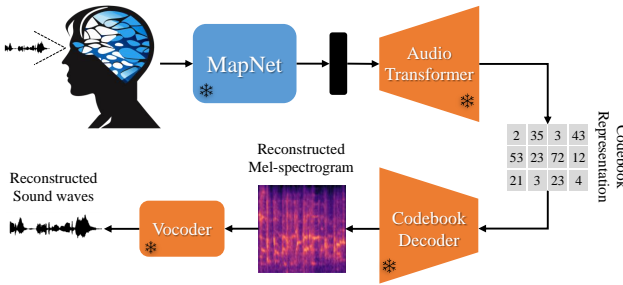


Figure 6. BSR [134]: State-of-the-art model for SBS tasks.

gressive decoder, employs Ridge regression to map fMRI voxels to semantic sound features. These Deep-Sound features are extracted from deep layers of a pretrained sound recognition DNN, which is performed on Mel-spectrograms of natural sound stimuli. The mapped semantic features are then fed into a pretrained audio transformer to generate codebook representation. The pretrained codebook decoder receives this representation and reproduces the Mel-spectrogram, subsequently converted in sound waves by a pretrained Vocoder, as depicted in Fig.6.

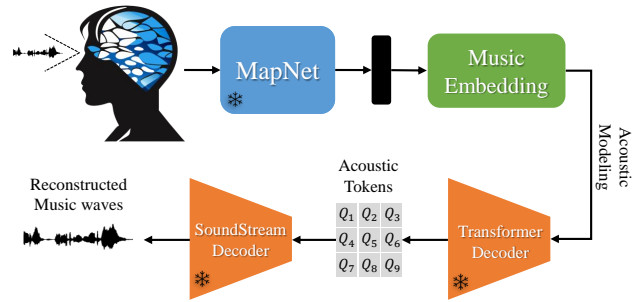


Figure 7. Brain2Music [39]: State-of-the-art model for MBM tasks.

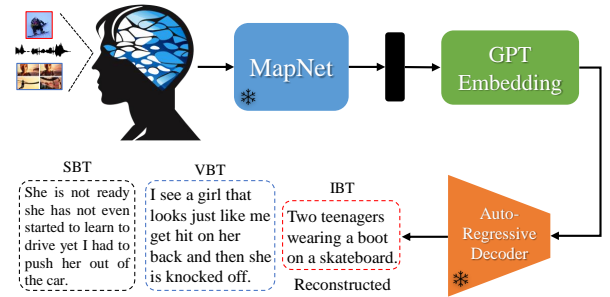


Figure 8. Representative framework for IBT, VBT, and SBT tasks.

6.4. Music-Brain-Music

For the MBM task, we have identified studies employing the Map and E2E methods. NDMusic adopts an end-to-end bidirectional LSTM (BiLSTM) architecture to establish a direct mapping from fMRI-informed EEG signals to music signals. In particular, Brain2Music follows the Map method, incorporating a mapping network based on Ridge regression and a pretrained AIGC decoder MusicLM [1]. The MusicLM model comprises three key components: i) w2v-BERT [30] for speech representation; ii) MuLan [72] for contrastive semantic representation in both audio and text domains; and iii) SoundStream [196], a neural audio codec, responsible for the generation of audio signals. Specifically, as illustrated in Fig.7, brain signals are mapped to music embedding (i.e., w2v-BERT tokens and MuLan embeddings) and decoded into acoustic tokens (latent representation in SoundStream with residual vector quantizer), which are sequentially decoded into music waves via the pretrained SoundStream decoder.

6.5. Image&Video&Speech-Brain-Text

The text generation task involves Map, BPM, MTF, and E2E methods with autoregressive decoders, except that Uni-Brain employs the diffusion decoder for both IBI and IBT tasks.

For the IBT task, BrainCaptioning maps fMRI vox-

els to CLIP-Image features using Ridge regression, which are then decoded into text by the Generative Image-to-text Transformer (GIT) [184]. DreamCatcher [18] utilizes FCN to map fMRI voxels to GPT embeddings and employs LSTM as an autoregressive decoder for text generation, as depicted in Fig.8. DSR [112] and GNLD [111] employ FCN and MLP to map fMRI voxels to visual features extracted from deep layers of VGG, respectively. Both of them use the autoregressive decoder LSTM for text generation. UniBrain [110] maps fMRI signals to low-level text detail priors (i.e., words and sentences), as well as semantic priors derived from CLIP-Text and CLIP-Image. The pretrained versatile diffusion (VD) decoder receives prior information and generates descriptive captions for image stimuli.

For the SBT task, UniCoRN [190] first performs brain pretraining using CAE to extract brain latent features, which are then mapped to the embedding of BART [97] via a projection network. Finally, BART embeddings are decoded into text by the pretrained BART decoder. CLSR [170] maps fMRI signals to the GPT embedding via Ridge regression and then decodes it into text by a pretrained GPT, as depicted in Fig.8. Furthermore, language features from this GPT embedding can transfer to the VBT task that helps to generate captions for silent video stimuli [169, 170].

6.6. Other Tasks

This survey mainly focuses on passive non-invasive AIGC-Brain tasks evoked by sensory stimuli (i.e., vision and audio) as described above, other AIGC-Brain generative tasks are briefly introduced as follows.

Active Tasks: In contrast to passive tasks, active AIGC-Brain tasks do not necessitate stimulus intervention during the inference stage, leveraging spontaneous brain signals to guide cross-modal content synthesis. This distinctive feature distinguishes them from passive tasks, showcasing the potential for self-driven cognitive processes in shaping multimodal information integration. Presently, we delineate two types of active brain-conditional tasks: i) Reading and Mental Rehearsal: Brain signals induced via reading text are utilized to synthesize semantic textual content, and participants are only required to actively rehearse the text mentally during the inference stage, termed Brain-to-Text [46]; ii) Imagery: Brain signals induced via the imagination of visual scenes or auditory content are utilized to synthesize multimodal content, and participants are only required to actively imagine relevant information during the inference stage. Associated generative tasks conditioned on imagery brain signals involve Brain-to-Image, Brain-to-Speech [170], and so on. For instance, Brain-to-Image refers to the ability to mentally generate or recall visual experiences without external sensory input. Several studies [117, 157, 171] have implemented EEG-based Brain-to-

Image tasks on the EEG-Imagey dataset [92], which is collected from 23 subjects imaging three different categories (characters, digits, and objects).

Invasive Tasks: While invasive techniques often provide more direct access to neural activity, they come with higher risks and ethical considerations due to the need for surgery. Currently, invasive neuroimaging techniques like ECoG (Electrocorticography) and intracranial EEG (iEEG) have been utilized for invasive AIGC-Brain tasks, involving Brain-to-Speech [3], Brain-to-Music [7], and so on.

7. AIGC-Brain Results

The purpose of AIGC-Brain tasks is to reconstruct the original stimulus or its textual description from the evoked brain signals. To this end, AIGC-Brain results need to focus on the fidelity between the ground truth and generated content, including low-level detail fidelity and high-level semantic fidelity. In this session, we will present qualitative results and quantitative metrics/results that have been summarized from representative datasets and models used for AIGC-Brain tasks. To be fair, we only provide performance comparisons for multiple works with the same dataset as well as the same experimental setup.

7.1. Qualitative Results

The qualitative results of representative models for all AIGC-Brain tasks are depicted in Fig.9. Generative content is selected from representative models and presented beside corresponding sensory stimuli. Specifically, Fig.9-A focuses on IBI qualitative results on GOD (left) and EEG-VOA (right) datasets. Image stimuli in both GOD and EEG-VOA are subsets from ImageNet. For EEG-VOA, all these models reproduce high semantic fidelity (i.e., panda, Jack-o-lantern, and airplane) and similar details in terms of object color and contour. However, generative results for GOD exhibit inadequate semantic or detail fidelity. For instance, SSRNIR generates images with high detail fidelity but is blurry. BrainICG and Mind-Vis generate realistic images but semantic mismatch (i.e., object category) and detail mismatch (i.e., object color) still exist. This phenomenon is mainly caused by the difficulty of zero-shot tests on GOD.

Fig.9-B focuses on IBI (left) and IBT (right) qualitative results on the NSD dataset. All these state-of-the-art models reproduce images with both high semantic (i.e., object relationship, scene understanding) and detail fidelity (i.e., pixel and contour). UniBrain [110] generates high-fidelity images and well-described captions from image-evoked brain signals, respectively.

Fig.9-C focuses on VBV qualitative results on the DNV dataset. SSRNM [93] and f-CVGAN [183] only reconstruct blurred video frames with rough object contours, which are not realistic enough. Mind-Video produces high-quality

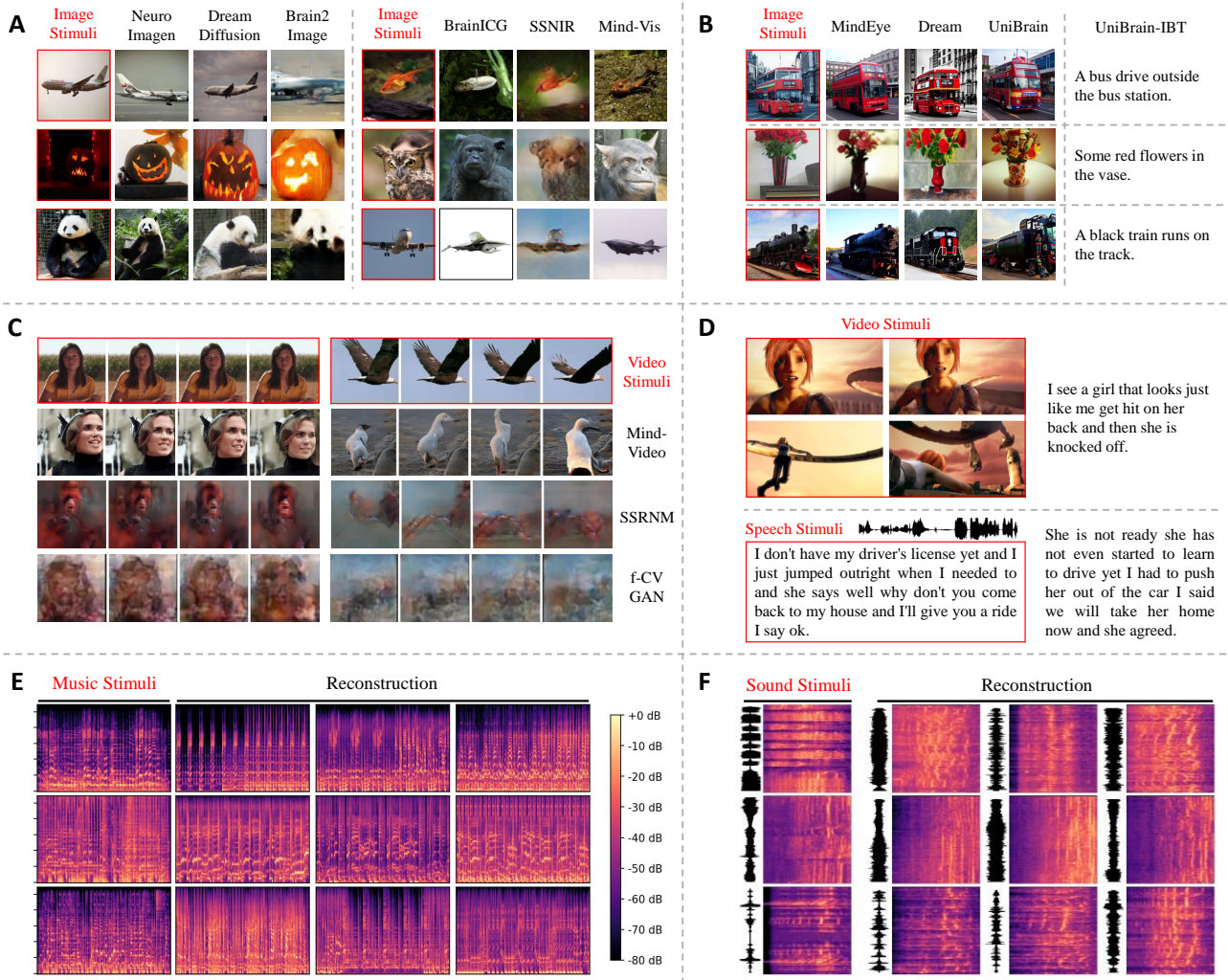


Figure 9. Qualitative Results for AIGC-Brain Tasks. A: IBI results on GOD (left) and EEG-VOA (right) datasets; B: IBI and IBT results on NSD dataset; C: VBV results on DNV dataset; D: VBT (top) and SBT (bottom) results based on CLSR [170]; E: MBM results based on Brain2Music [39]; F: SBS results based on BSR [134].

video frames while maintaining similar semantic information in terms of object category (i.e., woman and pigeon). However, the fidelity of details (i.e., pixel, contour, and motion vectors) still needs to be improved.

Fig.9-D focuses on VBT (top) and SBT (bottom) qualitative results based on the dataset and model from CLSR [170]. CLSR generates textual descriptions from brain signals evoked by video and speech stimuli. For VBT, the generated captions match the video scenes (i.e., object, motion) and connect them via the timeline (i.e., look, hit, and knock-off). For SBT, the generated language resembles the original speech content in semantics, even though there are differences in low-level text information (i.e., word and phrase).

Fig.9-E focuses on MBM qualitative results from Brain2Music [39] upon the MusicGenre dataset. The music stimuli and reconstruction samples are shown in the Mel-Spectrogram format. As can be seen, the generated Mel-Spectrograms exhibit similar spectral patterns to the original Mel-Spectrogram. Audio of more original and reconstructed music can be found in this project: <https://google-research.github.io/seanet/brain2music/>.

Fig.9-F focuses on SBS qualitative results based on the dataset and model from BSR [134]. The sound stimuli and reconstruction samples are shown in the waveform and Mel-Spectrogram formats. From top to bottom, sound stimuli are from chicken clucking, cow lowing, and donkey, respec-

Table 4. Quantitative Results of AIGC-Brain Models on the NSD Dataset for **IBI**.

Model	Low-Level				High-Level			
	PixCorr \uparrow	SSIM \uparrow	AlexNet-2 \uparrow	AlexNet-5 \uparrow	Inception \uparrow	CLIP \uparrow	EffNet \downarrow	SwAV \downarrow
Mind-Reader [102]	-	-	-	-	0.782	-	-	-
BrainSCN [61]	0.15	0.325	-	-	-	-	0.862	0.465
BrainSD [166]	-	-	0.83	0.83	0.76	0.77	-	-
BrainSD-TGD [167]	-	-	-	-	0.843	0.866	-	-
MindDiffuser [109]	-	0.354	-	-	-	-	-	-
BrainDiffuser [130]	0.254	0.356	0.942	0.962	0.872	0.915	0.775	0.423
BrainCLIP [105]	-	-	-	-	0.867	0.948	-	-
UniBrain [110]	0.249	0.330	0.929	0.956	0.878	0.923	0.766	0.407
MindEye [151]	0.309	0.323	0.947	0.978	0.938	0.941	0.645	0.367
Dream [191]	0.288	0.338	0.95	0.975	0.948	0.952	0.638	0.413

Table 5. Quantitative Results of AIGC-Brain Models on the GOD Dataset for **IBI**.

Model	Low-Level			High-Level			
	PixCorr \uparrow	SSIM \uparrow	PCC \uparrow	Inception-Dist \downarrow	CLIP-Dist \downarrow	SwAV \downarrow	ACC \uparrow
DIR [155]	0.339	0.539	-	0.933	0.379	0.581	-
SSNIR [6]	0.351	0.575	0.482	0.896	0.415	0.690	4.288
SSNIR-SC [54]	0.459	0.607	0.683	0.871	0.389	0.592	9.128
BrainBBG [120]	0.103	0.431	-	0.932	0.346	0.577	-
BrainDVG [145]	0.657	0.605	-	0.838	0.393	0.617	-
BrainICG [129]	0.223	0.453	0.449	0.846	0.340	0.510	29.386
BrainCLIP [105]	0.175	0.448	-	0.908	0.301	0.527	-
DBDM [113]	0.231	0.473	-	0.611	0.225	0.405	-
Mind-Vis [25]	-	0.527	0.532	-	-	-	26.644
CMVDM [198]	-	0.632	0.768	-	-	-	30.112

tively. As can be seen, some of the generated speech signals and Mel-Spectrograms exhibit similar waveform and spectral patterns to the original Mel-Spectrogram.

7.2. Quantitative Results

To quantitatively compare current models, we summarize various visual, auditory, and textual evaluation metrics in both low-level and high-level aspects that have been utilized in previous work.

7.2.1 Image Metric

In this session, we summarize image reconstruction metrics in low-level and high-level aspects performed on the EEG-image dataset (EEG-VOA) and two representative fMRI-image datasets (NSD and GOD).

Low-level: Low-level image features provide basic information about the visual content and structure of the image, measured by: i) **PixCorr:** Pixel-level correlation of reconstructed and ground-truth images; ii) **SSIM:** Structural Similarity Index [186]; iii) **MSE:** Mean square error; iv)

AlexNet: AlexNet-2 and AlexNet-5 are the 2-way comparisons of the second (early) and fifth (middle) layers of AlexNet [90], respectively; v) **PCC:** The Pearson Correlation Coefficient measures the strength of the linear relationship between the pixel values of the reconstructed image and the original image.

High-level: High-level image features capture semantic information, object relationships, and contextual understanding of the image, measured by: i) **Inception:** A two-way comparison of the last pooling layer of InceptionV3 [164]; ii) **CLIP:** A two-way comparison of the output layer of the CLIP-Image [138] model; iii) **EffNet, SwAV, Inception-Dist, CLIP-Dist:** Distance metrics gathered from EfficientNet-B1 [168], SwAV-ResNet50 [14], InceptionV3 [164] and CLIP-Image [138] models, respectively; iv) **IS:** Inception score measures the realism and diversity of the generated images; v) **IC:** Inception Classification Accuracy refers to the accuracy of a generative model in producing images that the pretrained Inception-v3 classification model correctly classifies; vi) **ACC:** The 50-way top-1 accuracy that measures the proportion of cor-

rectly classified samples from 50 possible classes, where the predicted class is the top prediction.

The quantitative results of AIGC-Brain models on NSD, GOD, and EEG-VOA datasets for the IBI task are presented in Table 4, 5, and 6, respectively. The up-arrow in the tables means higher is better, and the down-arrow is vice versa.

7.2.2 Video Metric

The main difference between video features and image features lies in the temporal aspect. Video features encompass both spatial and temporal information, capturing changes over time through elements like motion vectors and optical flow. We summarize video reconstruction metrics in low-level and high-level aspects performed on the representative fMRI-Video dataset DNV [188] in Table 7. Similar to image metrics, SSIM, MSE, and Peak Signal-to-Noise Ratio (PSNR) are used as low-level metrics, and ACC is used as high-level metrics. Furthermore, the Rank score is determined by computing the similarity of short reconstructed clips to n clips (including one correct and $n-1$ distractors) from the real test video, sorting the computed similarities, and assigning a score based on the position of the correct ground-truth clip within the sorted list, with a lower score indicating higher similarity [93]. However, these metrics are mainly focused on frame-based spatial and object category consistency, and sequence-based temporal consistency should be further considered. Temporal consistency among frames could be measured by Temporal Structural Similarity (t-SSIM), Temporal-Geometric Consistency (TGC), and Temporal-Geometric Consistency (TGC), etc.

7.2.3 Sound&Speech Metric

For sound reconstruction, the fidelity and quality of BSR [134] are assessed via an identification analysis that incorporates pixels of the Mel-spectrogram, hierarchical sound representation of DNN layers, and acoustic features like the fundamental frequency (F0), the spectral centroid (SC), and the harmonic to noise ratio (HNR). Experimental results demonstrated that the BSR model can not only reconstruct approximate spectral patterns but also the perceptual qualities akin to actual sound stimuli.

For speech reconstruction, ETCAS [62] measures the generative performance by ACC, PCC [31], and Mel-cepstral distance (MCD) [91]. Among them, PCC and MCD are low-level speech metrics, while the ACC serves as the high-level metric.

7.2.4 Music Metric

Brain2Music [39] evaluates generated music similarity using identification accuracy for two different levels of semantic abstraction and Top- n -class agreement. The latter em-

Table 6. Quantitative Results of AIGC-Brain Models on the EEG-VOA Dataset for IBI.

Model	Low-Level		High-Level	
	SSIM \uparrow	IS \uparrow	IC \uparrow	ACC \uparrow
Brain2Image [84]	-	5.070	0.430	-
EEG-GAN [132]	-	5.070	0.430	-
NeuroVision [86]	-	5.152	-	-
EEG-VGD [80]	-	6.330	0.530	-
DM-RE2I [199]	-	12.550	-	-
DreamDiffusion [4]	-	-	-	45.800
NeuroImagen [94]	0.249	33.500	-	85.600

Table 7. Quantitative Results of AIGC-Brain Models on the DNV Dataset for VBV.

Model	Low-Level			High-Level	
	SSIM \uparrow	MSE \downarrow	PSNR \uparrow	Rank \downarrow	ACC \uparrow
DNV [188]	0.16	0.090	-	34.200	-
f-CVGAN [183]	0.094	0.118	11.432	-	-
SSRNM (0.5Hz) [93]	0.102	0.136	-	7.180	-
SSRNM (4Hz) [93]	0.086	0.128	-	-	-
Mind-Video [26]	-	0.171	-	-	0.202

ploys the LEAF classifier [197] on AudioSet classes [56], calculating per-class probabilities for original and reconstructed music across genres, instruments, and moods. The top- n agreement measures the overlap between the top- n most probable class labels for the original and reconstructed music in each category. NDMusic [34] utilizes rank accuracy which refers to the measure of how accurately the music decoding process can identify the specific piece of music each participant was listening to in a trial. It involves assessing the similarity between the original and decoded music for an EEG trial and ranking this similarity against the similarity between the decoded music in that trial and the original music played in all other trials.

7.2.5 Text Metric

The evaluation of decoded text involved several automated low-level and high-level metrics for assessing text similarity.

Low-Level: Low-level text features provide basic information about the structure and composition of the text but do not capture the deeper meaning or semantic relationships between words, measured by: i) **Meteor:** The Meteor metric [5] provides a more robust evaluation by considering not only word overlap but also word order, synonymy, and other linguistic aspects that impact translation quality; ii) **Rouge:** Rouge-1 and Rouge-L [101] are specific variants of the Rouge (Recall-Oriented Understudy for Gisting Evaluation) metric that focus on capturing the similarity between the generated and reference summaries; iii) **BLEU:** BLEU [133] measures the precision of predicted n -grams

occurring in the reference sequence; iv) **WER**: Word Error Rate quantifies the number of edits (insertions, deletions, or substitutions) needed to transform the predicted sequence into the reference sequence.

High-Level: High-level text features are more complex and meaningful representations of text data that capture the context, relationships, and semantics of words and sentences, measured by: i) **CLIP**: A two-way comparison of the output layer of the CLIP-Text [138] model; ii) **BERTScore**: BERTScore [202] utilizes bidirectional transformer language models to represent words and computes a matching score; iii) **Sentence**: SentenceTransformer similarity score [144] is utilized to assess how well the generated text aligns semantically with a reference text.

The text generation metrics for AIGC-Brain models on representative datasets are summarized in Table 8, including AIGC-Brain tasks, datasets, models, and corresponding text metrics. We do not present the performance comparison of the models due to differences in the experimental settings, which would be unfair. For example, despite being under the same dataset, DreamCatcher and BrainCaptioning only use data from Subject-1 and Subject-2 in their experiments, while UniBrain utilizes data from all subjects (1, 2, 5, 7).

Table 8. Text Metrics for AIGC-Brain Text Synthesis Models.

Task	Dataset	Model	Text Metric
IBT	NSD	UniBrain [110]	Meteor, Rouge, CLIP
		DreamCatcher [18]	Meteor, Sentence, CLIP
		BrainCaptioning [51]	Meteor, Perplexity, Sentence
	OCD	GIC-PTL [73]	Rouge
GIC-CT [200]		Rouge	
SBT&VBT	CLSR	CLSR [170]	WER, BLEU, Meteor, BERTScore

8. Conclusions and Prospects

This investigation systematically summarizes the research foundation and recent advancement in the AIGC-Brain domain. On the one hand, the research foundation includes relevant neuroimaging datasets, functional brain regions, and generative models in the mainstream AIGC field. On the other hand, we introduce a taxonomy based on distinctions in model implementation architectures, emphasizing workflows, mapping relationships, and the merits and demerits of each method. This taxonomy serves to delineate the current methodological landscape for AIGC-Brain technologies. Subsequently, we delve into task-specific representative work and implementation details, facilitating a comparative analysis of technological trends, task-specific characteristics, and preferences. To orient researchers to the forefront of the field, we outline cutting-edge work and frameworks for each task. Additionally, we summarize quality assessment methodologies, covering both qualitative and quantitative dimensions, and showcase perfor-

mance comparisons on representative datasets for reference. In essence, this survey navigates from the research foundational of AIGC-Brain, through methodology taxonomy, task-specific implementations, and state-of-the-art advancements, to the evaluation of model performance. It furnishes researchers in the field with a comprehensive research continuum, establishing a robust foundation for subsequent technological developments. Moving forward, we discuss the challenges impeding current AIGC-Brain technological advancements and offer insights into potential directions for future developments as follows:

Data: Non-invasive neuroimaging data are generally characterized by low signal-to-noise ratio and high variability, making it difficult to learn and generalize. Moreover, different neuroimaging technologies exhibit preferences for specific types of information, e.g., fMRI emphasizes detailed spatial mapping, EEG prioritizes high temporal resolution, and MEG combines both spatial and temporal information, but neither aspect is prominent. Neuroimaging datasets are basically small in scale due to the complexity and difficulty of neural data acquisition, posing challenges for the application of deep neural networks. Advancements in neuroimaging technology and the availability of larger datasets will contribute to the progress of AIGC-Brain technology.

Fidelity: Unlike the AIGC field, which emphasizes the diversity of generated results, passive brain condition multimodal synthesis content needs to be consistent with the perception received by the brain. That is, generated results in the AIGC-Brain domain are more concerned with detail and semantic fidelity. To this end, future work requires improved cross-modal matching and high-quality generation capabilities in both low-level and high-level aspects.

Flexibility: Flexibility refers to model adaptation and the capability of transferring to different datasets and tasks. For instance, the flexibility of the Map method is significantly greater than that of the BPFA method, which is reflected in: i) The cost of training for the Map method is minimal, whereas BPFA necessitates extensive pretraining and finetuning of the deep generative model; ii) The Map method can flexibly incorporate various prior information or modify the pretrained AIGC decoder to enhance model performance; iii) The Map method is not limited by data variances (e.g., different neuroimaging type and length, etc.), while the BPFA method needs to ensure similarity between upstream pretraining data and downstream data. Overall, Improving model flexibility contributes to model generalization and technology updates.

Interpretability: Decoding brain signals back to perceptual information contributes to unraveling the mechanisms underlying how the brain perceives and comprehends external stimuli. Hence, interpretability is crucial. It is imperative to observe the activation and coordination patterns

across various brain regions during the decoding process, as well as dynamic changes. For instance, in the reception of visual information, brain activation regions transition from the low visual cortex (LVC) to the high visual cortex (HVC). Interpretability of AIGC-Brain technologies enhances our understanding of the neural processes involved in decoding sensory information.

Real-time: Given the application of AIGC-Brain technology in BCI systems, real-time processing emerges as a crucial practical consideration. BCI systems necessitate the real-time capabilities of decoding models to achieve online responsiveness and provide instantaneous feedback.

Multimodality: The human brain establishes a One-to-Many relationship between brain modalities and external modalities, as exemplified by brain signals elicited from video stimuli corresponding to video, sound, and text modalities. Furthermore, the perceptual experience in the brain encompasses not only the stimulus itself but also associative information. For instance, upon seeing a photo of a bird, the brain can establish connections with the sound of a bird’s call. Therefore, brain signals can concurrently establish connections with multiple external modalities. To the best of our knowledge, among existing AIGC-Brain models, only UniBrain is multimodal, employing a unified AIGC-Brain decoder to simultaneously decode images and text from brain signals elicited by visual stimuli. Looking ahead, we anticipate the emergence of a unified **Brain-to-Any** multimodal synthesis model.

References

- [1] Andrea Agostinelli, Timo I Denk, Zalan Borsos, Jesse Engel, Mauro Verzetti, Antoine Caillon, Qingqing Huang, Aren Jansen, Adam Roberts, Marco Tagliasacchi, et al. Musiclm: Generating music from text. *arXiv preprint arXiv:2301.11325*, 2023.
- [2] Emily J Allen, Ghislain St-Yves, Yihan Wu, Jesse L Breedlove, Jacob S Prince, Logan T Dowdle, Matthias Nau, Brad Caron, Franco Pestilli, Ian Charest, et al. A massive 7t fmri dataset to bridge cognitive neuroscience and artificial intelligence. *Nature neuroscience*, 25(1):116–126, 2022.
- [3] Gopala K Anumanchipalli, Josh Chartier, and Edward F Chang. Speech synthesis from neural decoding of spoken sentences. *Nature*, 568(7753):493–498, 2019.
- [4] Yunpeng Bai, Xintao Wang, Yanpei Cao, Yixiao Ge, Chun Yuan, and Ying Shan. Dreamdiffusion: Generating high-quality images from brain eeg signals. *arXiv preprint arXiv:2306.16934*, 2023.
- [5] Satanjeev Banerjee and Alon Lavie. Meteor: An automatic metric for mt evaluation with improved correlation with human judgments. In *Proceedings of the acl workshop on intrinsic and extrinsic evaluation measures for machine translation and/or summarization*, pages 65–72, 2005.
- [6] Roman Belyi, Guy Gaziv, Assaf Hoogi, Francesca Strappini, Tal Golan, and Michal Irani. From voxels to pixels and back: Self-supervision in natural-image reconstruction from fmri. *Advances in Neural Information Processing Systems*, 32, 2019.
- [7] Ludovic Bellier, Anaïs Llorens, Déborah Marciano, Aysegül Gunduz, Gerwin Schalk, Peter Brunner, and Robert T Knight. Music can be reconstructed from human auditory cortex activity using nonlinear decoding models. *PLoS biology*, 21(8):e3002176, 2023.
- [8] Johann Banchetrit, Hubert Banville, and Jean-Rémi King. Brain decoding: toward real-time reconstruction of visual perception. *arXiv preprint arXiv:2310.19812*, 2023.
- [9] Mikołaj Bińkowski, Jeff Donahue, Sander Dieleman, Aidan Clark, Erich Elsen, Norman Casagrande, Luis C Cobo, and Karen Simonyan. High fidelity speech synthesis with adversarial networks. *arXiv preprint arXiv:1909.11646*, 2019.
- [10] Andreas Blattmann, Tim Dockhorn, Sumith Kulal, Daniel Mendelevitch, Maciej Kilian, Dominik Lorenz, Yam Levi, Zion English, Vikram Voleti, Adam Letts, et al. Stable video diffusion: Scaling latent video diffusion models to large datasets. *arXiv preprint arXiv:2311.15127*, 2023.
- [11] Alyssa A Brewer and Brian Barton. Maps of the auditory cortex. *Annual review of neuroscience*, 39:385–407, 2016.
- [12] Tom Brown, Benjamin Mann, Nick Ryder, Melanie Subbiah, Jared D Kaplan, Prafulla Dhariwal, Arvind Neelakantan, Pranav Shyam, Girish Sastry, Amanda Askell, et al. Language models are few-shot learners. *Advances in neural information processing systems*, 33:1877–1901, 2020.
- [13] Sébastien Bubeck, Varun Chandrasekaran, Ronen Eldan, Johannes Gehrke, Eric Horvitz, Ece Kamar, Peter Lee, Yin Tat Lee, Yuanzhi Li, Scott Lundberg, et al. Sparks of artificial general intelligence: Early experiments with gpt-4. *arXiv preprint arXiv:2303.12712*, 2023.
- [14] Mathilde Caron, Ishan Misra, Julien Mairal, Priya Goyal, Piotr Bojanowski, and Armand Joulin. Unsupervised learning of visual features by contrasting cluster assignments. *Advances in neural information processing systems*, 33:9912–9924, 2020.
- [15] Arantxa Casanova, Marlene Careil, Jakob Verbeek, Michal Drozdal, and Adriana Romero Soriano. Instance-conditioned gan. *Advances in Neural Information Processing Systems*, 34:27517–27529, 2021.
- [16] Huiwen Chang, Han Zhang, Lu Jiang, Ce Liu, and William T Freeman. Maskgit: Masked generative image transformer. In *Proceedings of the IEEE/CVF Conference on Computer Vision and Pattern Recognition*, pages 11315–11325, 2022.
- [17] Nadine Chang, John A Pyles, Austin Marcus, Abhinav Gupta, Michael J Tarr, and Elissa M Aminoff. Bold5000, a public fmri dataset while viewing 5000 visual images. *Scientific data*, 6(1):49, 2019.
- [18] Subhrasankar Chatterjee and Debasis Samanta. Dreamcatcher: Revealing the language of the brain with fmri using gpt embedding. *arXiv preprint arXiv:2306.10082*, 2023.
- [19] Honglie Chen, Weidi Xie, Andrea Vedaldi, and Andrew Zisserman. Vggsound: A large-scale audio-visual dataset. In *ICASSP 2020-2020 IEEE International Conference on Acoustics, Speech and Signal Processing (ICASSP)*, pages 721–725. IEEE, 2020.

- [20] Jiaxuan Chen, Yu Qi, and Gang Pan. Rethinking visual reconstruction: Experience-based content completion guided by visual cues. In Andreas Krause, Emma Brunskill, Kyunghyun Cho, Barbara Engelhardt, Sivan Sabato, and Jonathan Scarlett, editors, *Proceedings of the 40th International Conference on Machine Learning*, volume 202 of *Proceedings of Machine Learning Research*, pages 4856–4866. PMLR, 23–29 Jul 2023.
- [21] Mark Chen, Alec Radford, Rewon Child, Jeffrey Wu, Heewoo Jun, David Luan, and Ilya Sutskever. Generative pre-training from pixels. In *International conference on machine learning*, pages 1691–1703. PMLR, 2020.
- [22] Xi Chen, Yan Duan, Rein Houthoofd, John Schulman, Ilya Sutskever, and Pieter Abbeel. Infogan: Interpretable representation learning by information maximizing generative adversarial nets. *Advances in neural information processing systems*, 29, 2016.
- [23] X Chen, S Xie, and K He. An empirical study of training self-supervised vision transformers. In *CVF International Conference on Computer Vision (ICCV)*, pages 9620–9629, 2021.
- [24] Xiaogang Chen, Bing Zhao, Yijun Wang, and Xiaorong Gao. Combination of high-frequency ssvp-based bci and computer vision for controlling a robotic arm. *Journal of neural engineering*, 16(2):026012, 2019.
- [25] Zijiao Chen, Jiaxin Qing, Tiange Xiang, Wan Lin Yue, and Juan Helen Zhou. Seeing beyond the brain: Conditional diffusion model with sparse masked modeling for vision decoding. In *Proceedings of the IEEE/CVF Conference on Computer Vision and Pattern Recognition*, pages 22710–22720, 2023.
- [26] Zijiao Chen, Jiaxin Qing, and Juan Helen Zhou. Cinematic mindscapes: High-quality video reconstruction from brain activity. *arXiv preprint arXiv:2305.11675*, 2023.
- [27] Zhengxue Cheng, Heming Sun, Masaru Takeuchi, and Jiro Katto. Deep convolutional autoencoder-based lossy image compression. In *2018 Picture Coding Symposium (PCS)*, pages 253–257. IEEE, 2018.
- [28] Ching-Yu Chiu, Avinash K Singh, Yu-Kai Wang, Jung-Tai King, and Chin-Teng Lin. A wireless steady state visually evoked potential-based bci eating assistive system. In *2017 International Joint Conference on Neural Networks (IJCNN)*, pages 3003–3007. IEEE, 2017.
- [29] Kyunghyun Cho, Bart Van Merriënboer, Caglar Gulcehre, Dzmitry Bahdanau, Fethi Bougares, Holger Schwenk, and Yoshua Bengio. Learning phrase representations using rnn encoder-decoder for statistical machine translation. *arXiv preprint arXiv:1406.1078*, 2014.
- [30] Yu-An Chung, Yu Zhang, Wei Han, Chung-Cheng Chiu, James Qin, Ruoming Pang, and Yonghui Wu. W2v-bert: Combining contrastive learning and masked language modeling for self-supervised speech pre-training. In *2021 IEEE Automatic Speech Recognition and Understanding Workshop (ASRU)*, pages 244–250. IEEE, 2021.
- [31] Israel Cohen, Yiteng Huang, Jingdong Chen, Jacob Benesty, Jacob Benesty, Jingdong Chen, Yiteng Huang, and Israel Cohen. Pearson correlation coefficient. *Noise reduction in speech processing*, pages 1–4, 2009.
- [32] Michael X Cohen. Where does eeg come from and what does it mean? *Trends in neurosciences*, 40(4):208–218, 2017.
- [33] Fernando Lopes da Silva. Eeg and meg: relevance to neuroscience. *Neuron*, 80(5):1112–1128, 2013.
- [34] Ian Daly. Neural decoding of music from the eeg. *Scientific Reports*, 13(1):624, 2023.
- [35] Ian Daly, Nicoletta Nicolaou, Duncan Williams, Faustina Hwang, Alexis Kirke, Eduardo Miranda, and Slawomir J Nasuto. Neural and physiological data from participants listening to affective music. *Scientific Data*, 7(1):177, 2020.
- [36] Alexandre Défossez, Charlotte Caucheteux, Jérémy Rapin, Ori Kabeli, and Jean-Rémi King. Decoding speech perception from non-invasive brain recordings. *Nature Machine Intelligence*, pages 1–11, 2023.
- [37] Alexander Degerman, Teemu Rinne, Johanna Pekkola, Taina Autti, Iiro P Jääskeläinen, Mikko Sams, and Kimmo Alho. Human brain activity associated with audiovisual perception and attention. *Neuroimage*, 34(4):1683–1691, 2007.
- [38] Jia Deng, Wei Dong, Richard Socher, Li-Jia Li, Kai Li, and Li Fei-Fei. Imagenet: A large-scale hierarchical image database. In *2009 IEEE conference on computer vision and pattern recognition*, pages 248–255. Ieee, 2009.
- [39] Timo I Denk, Yu Takagi, Takuya Matsuyama, Andrea Agostinelli, Tomoya Nakai, Christian Frank, and Shinji Nishimoto. Brain2music: Reconstructing music from human brain activity. *arXiv preprint arXiv:2307.11078*, 2023.
- [40] Prafulla Dhariwal and Alexander Nichol. Diffusion models beat gans on image synthesis. *Advances in neural information processing systems*, 34:8780–8794, 2021.
- [41] Prafulla Dhariwal and Alexander Nichol. Diffusion models beat gans on image synthesis. *Advances in neural information processing systems*, 34:8780–8794, 2021.
- [42] Ming Ding, Zhuoyi Yang, Wenyi Hong, Wendi Zheng, Chang Zhou, Da Yin, Junyang Lin, Xu Zou, Zhou Shao, Hongxia Yang, et al. Cogview: Mastering text-to-image generation via transformers. *Advances in Neural Information Processing Systems*, 34:19822–19835, 2021.
- [43] Chris Donahue, Julian McAuley, and Miller Puckette. Adversarial audio synthesis. *arXiv preprint arXiv:1802.04208*, 2018.
- [44] Jeff Donahue and Karen Simonyan. Large scale adversarial representation learning. *Advances in neural information processing systems*, 32, 2019.
- [45] Changde Du, Kaicheng Fu, Jinpeng Li, and Huiguang He. Decoding visual neural representations by multimodal learning of brain-visual-linguistic features. *IEEE Transactions on Pattern Analysis and Machine Intelligence*, 2023.
- [46] Yiqun Duan, Jinzhao Zhou, Zhen Wang, Yu-Kai Wang, and Chin-Teng Lin. Dewave: Discrete eeg waves encoding for brain dynamics to text translation. *arXiv preprint arXiv:2309.14030*, 2023.
- [47] Patrick Esser, Robin Rombach, Andreas Blattmann, and Bjorn Ommer. Imagebart: Bidirectional context with multinomial diffusion for autoregressive image synthesis. *Advances in neural information processing systems*, 34:3518–3532, 2021.

- [48] Patrick Esser, Robin Rombach, and Bjorn Ommer. Taming transformers for high-resolution image synthesis. In *Proceedings of the IEEE/CVF conference on computer vision and pattern recognition*, pages 12873–12883, 2021.
- [49] Tao Fang, Yu Qi, and Gang Pan. Reconstructing perceptive images from brain activity by shape-semantic gan. *Advances in Neural Information Processing Systems*, 33:13038–13048, 2020.
- [50] Matteo Ferrante, Tommaso Boccato, and Nicola Toschi. Semantic brain decoding: from fmri to conceptually similar image reconstruction of visual stimuli. *arXiv preprint arXiv:2212.06726*, 2022.
- [51] Matteo Ferrante, Furkan Ozcelik, Tommaso Boccato, Rufin VanRullen, and Nicola Toschi. Brain captioning: Decoding human brain activity into images and text. *arXiv preprint arXiv:2305.11560*, 2023.
- [52] Karl J Friston. Models of brain function in neuroimaging. *Annu. Rev. Psychol.*, 56:57–87, 2005.
- [53] Giorgio Ganis, William L Thompson, and Stephen M Kosslyn. Brain areas underlying visual mental imagery and visual perception: an fmri study. *Cognitive Brain Research*, 20(2):226–241, 2004.
- [54] Guy Gaziv, Roman Belyi, Niv Granot, Assaf Hoogi, Francesca Strappini, Tal Golan, and Michal Irani. Self-supervised natural image reconstruction and large-scale semantic classification from brain activity. *NeuroImage*, 254:119121, 2022.
- [55] Guy Gaziv and Michal Irani. More than meets the eye: Self-supervised depth reconstruction from brain activity. *arXiv preprint arXiv:2106.05113*, 2021.
- [56] Jort F Gemmeke, Daniel PW Ellis, Dylan Freedman, Aren Jansen, Wade Lawrence, R Channing Moore, Manoj Plakal, and Marvin Ritter. Audio set: An ontology and human-labeled dataset for audio events. In *2017 IEEE international conference on acoustics, speech and signal processing (ICASSP)*, pages 776–780. IEEE, 2017.
- [57] Charles D Gilbert and Mariano Sigman. Brain states: top-down influences in sensory processing. *Neuron*, 54(5):677–696, 2007.
- [58] Rohit Girdhar, Alaaeldin El-Nouby, Zhuang Liu, Mannat Singh, Kalyan Vasudev Alwala, Armand Joulin, and Ishan Misra. Imagebind: One embedding space to bind them all. In *Proceedings of the IEEE/CVF Conference on Computer Vision and Pattern Recognition*, pages 15180–15190, 2023.
- [59] Ian Goodfellow, Jean Pouget-Abadie, Mehdi Mirza, Bing Xu, David Warde-Farley, Sherjil Ozair, Aaron Courville, and Yoshua Bengio. Generative adversarial networks. *Communications of the ACM*, 63(11):139–144, 2020.
- [60] Kalanit Grill-Spector and Rafael Malach. The human visual cortex. *Annu. Rev. Neurosci.*, 27:649–677, 2004.
- [61] Zijin Gu, Keith Jamison, Amy Kuceyeski, and Mert Sabuncu. Decoding natural image stimuli from fmri data with a surface-based convolutional network. *arXiv preprint arXiv:2212.02409*, 2022.
- [62] Yina Guo, Ting Liu, Xiaofei Zhang, Anhong Wang, and Wenwu Wang. End-to-end translation of human neural activity to speech with a dual–dual generative adversarial network. *Knowledge-Based Systems*, 277:110837, 2023.
- [63] Kuan Han, Haiguang Wen, Junxing Shi, Kun-Han Lu, Yizhen Zhang, Di Fu, and Zhongming Liu. Variational autoencoder: An unsupervised model for encoding and decoding fmri activity in visual cortex. *NeuroImage*, 198:125–136, 2019.
- [64] Kaiming He, Xinlei Chen, Saining Xie, Yanghao Li, Piotr Dollár, and Ross Girshick. Masked autoencoders are scalable vision learners. In *Proceedings of the IEEE/CVF conference on computer vision and pattern recognition*, pages 16000–16009, 2022.
- [65] Kaiming He, Xiangyu Zhang, Shaoqing Ren, and Jian Sun. Deep residual learning for image recognition. In *Proceedings of the IEEE conference on computer vision and pattern recognition*, pages 770–778, 2016.
- [66] Martin N Hebart, Oliver Contier, Lina Teichmann, Adam H Rockter, Charles Y Zheng, Alexis Kidder, Anna Corriveau, Maryam Vaziri-Pashkam, and Chris I Baker. Things-data, a multimodal collection of large-scale datasets for investigating object representations in human brain and behavior. *Elife*, 12:e82580, 2023.
- [67] Martin N Hebart, Adam H Dickter, Alexis Kidder, Wan Y Kwok, Anna Corriveau, Caitlin Van Wicklin, and Chris I Baker. Things: A database of 1,854 object concepts and more than 26,000 naturalistic object images. *PloS one*, 14(10):e0223792, 2019.
- [68] David J Heeger and David Ress. What does fmri tell us about neuronal activity? *Nature reviews neuroscience*, 3(2):142–151, 2002.
- [69] Jonathan Ho, Ajay Jain, and Pieter Abbeel. Denoising diffusion probabilistic models. *Advances in neural information processing systems*, 33:6840–6851, 2020.
- [70] Sepp Hochreiter and Jürgen Schmidhuber. Long short-term memory. *Neural computation*, 9(8):1735–1780, 1997.
- [71] Tomoyasu Horikawa and Yukiyasu Kamitani. Generic decoding of seen and imagined objects using hierarchical visual features. *Nature communications*, 8(1):15037, 2017.
- [72] Qingqing Huang, Aren Jansen, Joonseok Lee, Ravi Ganti, Judith Yue Li, and Daniel PW Ellis. Mulan: A joint embedding of music audio and natural language. *arXiv preprint arXiv:2208.12415*, 2022.
- [73] Wei Huang, Hongmei Yan, Kaiwen Cheng, Chong Wang, Jiyi Li, Yuting Wang, Chen Li, Chaorong Li, Yunhan Li, Zhentao Zuo, et al. A neural decoding algorithm that generates language from visual activity evoked by natural images. *Neural Networks*, 144:90–100, 2021.
- [74] Wei Huang, Hongmei Yan, Chong Wang, Jiyi Li, Xiaoqing Yang, Liang Li, Zhentao Zuo, Jiang Zhang, and Huaifu Chen. Long short-term memory-based neural decoding of object categories evoked by natural images. *Human Brain Mapping*, 41(15):4442–4453, 2020.
- [75] Phillip Isola, Jun-Yan Zhu, Tinghui Zhou, and Alexei A Efros. Image-to-image translation with conditional adversarial networks. In *Proceedings of the IEEE conference on computer vision and pattern recognition*, pages 1125–1134, 2017.
- [76] Phillip Isola, Jun-Yan Zhu, Tinghui Zhou, and Alexei A Efros. Image-to-image translation with conditional adversarial networks. In *Proceedings of the IEEE conference on*

- computer vision and pattern recognition*, pages 1125–1134, 2017.
- [77] Phillip Isola, Jun-Yan Zhu, Tinghui Zhou, and Alexei A Efros. Image-to-image translation with conditional adversarial networks. In *Proceedings of the IEEE conference on computer vision and pattern recognition*, pages 1125–1134, 2017.
- [78] Vinay Jayaram and Alexandre Barachant. Moabb: trustworthy algorithm benchmarking for bcis. *Journal of neural engineering*, 15(6):066011, 2018.
- [79] Yujin Jeong, Wonjeong Ryoo, Seunghyun Lee, Dabin Seo, Wonmin Byeon, Sangpil Kim, and Jinkyu Kim. The power of sound (tpos): Audio reactive video generation with stable diffusion. In *Proceedings of the IEEE/CVF International Conference on Computer Vision*, pages 7822–7832, 2023.
- [80] Zhicheng Jiao, Haoxuan You, Fan Yang, Xin Li, Han Zhang, and Dinggang Shen. Decoding eeg by visual-guided deep neural networks. In *Proceedings of the Twenty-Eighth International Joint Conference on Artificial Intelligence, IJCAI-19*, pages 1387–1393, 2019.
- [81] Tero Karras, Timo Aila, Samuli Laine, and Jaakko Lehtinen. Progressive growing of gans for improved quality, stability, and variation. *arXiv preprint arXiv:1710.10196*, 2017.
- [82] Tero Karras, Samuli Laine, and Timo Aila. A style-based generator architecture for generative adversarial networks. In *Proceedings of the IEEE/CVF conference on computer vision and pattern recognition*, pages 4401–4410, 2019.
- [83] Tero Karras, Samuli Laine, Miika Aittala, Janne Hellsten, Jaakko Lehtinen, and Timo Aila. Analyzing and improving the image quality of stylegan. In *Proceedings of the IEEE/CVF conference on computer vision and pattern recognition*, pages 8110–8119, 2020.
- [84] Isaak Kavasidis, Simone Palazzo, Concetto Spampinato, Daniela Giordano, and Mubarak Shah. Brain2image: Converting brain signals into images. In *Proceedings of the 25th ACM international conference on Multimedia*, pages 1809–1817, 2017.
- [85] Kendrick N Kay, Thomas Naselaris, Ryan J Prenger, and Jack L Gallant. Identifying natural images from human brain activity. *Nature*, 452(7185):352–355, 2008.
- [86] Sanchita Khare, Rajiv Nayan Choubey, Loveleen Amar, and Venkanna Udutalappalli. Neurovision: perceived image regeneration using cprogan. *Neural Computing and Applications*, 34(8):5979–5991, 2022.
- [87] Diederik P Kingma and Max Welling. Auto-encoding variational bayes. *arXiv preprint arXiv:1312.6114*, 2013.
- [88] Dan Kondratyuk, Lijun Yu, Xiuye Gu, José Lezama, Jonathan Huang, Rachel Hornung, Hartwig Adam, Hassan Akbari, Yair Alon, Vighnesh Birodkar, et al. Videopoet: A large language model for zero-shot video generation. *arXiv preprint arXiv:2312.14125*, 2023.
- [89] Mark A Kramer. Autoassociative neural networks. *Computers & chemical engineering*, 16(4):313–328, 1992.
- [90] Alex Krizhevsky, Ilya Sutskever, and Geoffrey E Hinton. Imagenet classification with deep convolutional neural networks. *Advances in neural information processing systems*, 25, 2012.
- [91] Robert Kubichek. Mel-cepstral distance measure for objective speech quality assessment. In *Proceedings of IEEE pacific rim conference on communications computers and signal processing*, volume 1, pages 125–128. IEEE, 1993.
- [92] Pradeep Kumar, Rajkumar Saini, Partha Pratim Roy, Pawan Kumar Sahu, and Debi Prosad Dogra. Envisioned speech recognition using eeg sensors. *Personal and Ubiquitous Computing*, 22:185–199, 2018.
- [93] Ganit Kupersmidt, Roman Belyi, Guy Gaziv, and Michal Irani. A penny for your (visual) thoughts: Self-supervised reconstruction of natural movies from brain activity. *arXiv preprint arXiv:2206.03544*, 2022.
- [94] Yu-Ting Lan, Kan Ren, Yansen Wang, Wei-Long Zheng, Dongsheng Li, Bao-Liang Lu, and Lili Qiu. Seeing through the brain: Image reconstruction of visual perception from human brain signals. *arXiv preprint arXiv:2308.02510*, 2023.
- [95] Anders Boesen Lindbo Larsen, Søren Kaae Sønderby, Hugo Larochelle, and Ole Winther. Autoencoding beyond pixels using a learned similarity metric. In *International conference on machine learning*, pages 1558–1566. PMLR, 2016.
- [96] Lynn Le, Luca Ambrogioni, Katja Seeliger, Yağmur Güçlütürk, Marcel van Gerven, and Umut Güçlü. Brain2pix: Fully convolutional naturalistic video frame reconstruction from brain activity. *Frontiers in Neuroscience*, 16:940972, 2022.
- [97] Mike Lewis, Yinhan Liu, Naman Goyal, Marjan Ghazvininejad, Abdelrahman Mohamed, Omer Levy, Ves Stoyanov, and Luke Zettlemoyer. Bart: Denoising sequence-to-sequence pre-training for natural language generation, translation, and comprehension. *arXiv preprint arXiv:1910.13461*, 2019.
- [98] Junnan Li, Dongxu Li, Silvio Savarese, and Steven Hoi. Blip-2: Bootstrapping language-image pre-training with frozen image encoders and large language models. *arXiv preprint arXiv:2301.12597*, 2023.
- [99] Junnan Li, Dongxu Li, Caiming Xiong, and Steven Hoi. Blip: Bootstrapping language-image pre-training for unified vision-language understanding and generation. In *International Conference on Machine Learning*, pages 12888–12900. PMLR, 2022.
- [100] Jeffrey Lim, Derrick Lin, Won Joon Sohn, Colin M McCrimmon, Po T Wang, Zoran Nenadic, and An H Do. Bci-based neuroprostheses and physiotherapies for stroke motor rehabilitation. In *Neurorehabilitation Technology*, pages 509–524. Springer, 2022.
- [101] Chin-Yew Lin. Rouge: A package for automatic evaluation of summaries. In *Text summarization branches out*, pages 74–81, 2004.
- [102] Sikun Lin, Thomas Sprague, and Ambuj K Singh. Mind reader: Reconstructing complex images from brain activities. *Advances in Neural Information Processing Systems*, 35:29624–29636, 2022.
- [103] Tsung-Yi Lin, Michael Maire, Serge Belongie, James Hays, Pietro Perona, Deva Ramanan, Piotr Dollár, and C Lawrence Zitnick. Microsoft coco: Common objects in

- context. In *Computer Vision—ECCV 2014: 13th European Conference, Zurich, Switzerland, September 6–12, 2014, Proceedings, Part V 13*, pages 740–755. Springer, 2014.
- [104] Haohe Liu, Zehua Chen, Yi Yuan, Xinhao Mei, Xubo Liu, Danilo Mandic, Wenwu Wang, and Mark D Plumbley. Audioldm: Text-to-audio generation with latent diffusion models. *arXiv preprint arXiv:2301.12503*, 2023.
- [105] Yulong Liu, Yongqiang Ma, Wei Zhou, Guibo Zhu, and Nanning Zheng. Brainclip: Bridging brain and visual-linguistic representation via clip for generic natural visual stimulus decoding from fmri. *arXiv preprint arXiv:2302.12971*, 2023.
- [106] Ziwei Liu, Ping Luo, Xiaogang Wang, and Xiaoou Tang. Deep learning face attributes in the wild. In *Proceedings of the IEEE international conference on computer vision*, pages 3730–3738, 2015.
- [107] Nikos K Logothetis, Jon Pauls, Mark Augath, Torsten Trinath, and Axel Oeltermann. Neurophysiological investigation of the basis of the fmri signal. *nature*, 412(6843):150–157, 2001.
- [108] Jiasen Lu, Christopher Clark, Sangho Lee, Zichen Zhang, Savya Khosla, Ryan Marten, Derek Hoiem, and Anirudha Kembhavi. Unified-io 2: Scaling autoregressive multimodal models with vision, language, audio, and action. *arXiv preprint arXiv:2312.17172*, 2023.
- [109] Yizhuo Lu, Changde Du, Dianpeng Wang, and Huiguang He. Minddiffuser: Controlled image reconstruction from human brain activity with semantic and structural diffusion. *arXiv preprint arXiv:2303.14139*, 2023.
- [110] Weijian Mai and Zhijun Zhang. Unibrain: Unify image reconstruction and captioning all in one diffusion model from human brain activity. *arXiv preprint arXiv:2308.07428*, 2023.
- [111] Eri Matsuo, Ichiro Kobayashi, Shinji Nishimoto, Satoshi Nishida, and Hideki Asoh. Generating natural language descriptions for semantic representations of human brain activity. In *Proceedings of the ACL 2016 student research workshop*, pages 22–29, 2016.
- [112] Eri Matsuo, Ichiro Kobayashi, Shinji Nishimoto, Satoshi Nishida, and Hideki Asoh. Describing semantic representations of brain activity evoked by visual stimuli. In *2018 IEEE International Conference on Systems, Man, and Cybernetics (SMC)*, pages 576–583. IEEE, 2018.
- [113] Lu Meng and Chuanhao Yang. Dual-guided brain diffusion model: Natural image reconstruction from human visual stimulus fmri. *Bioengineering*, 10(10):1117, 2023.
- [114] Lu Meng and Chuanhao Yang. Semantics-guided hierarchical feature encoding generative adversarial network for natural image reconstruction from brain activities. In *2023 International Joint Conference on Neural Networks (IJCNN)*, pages 1–9. IEEE, 2023.
- [115] Martin Meyer, Simon Baumann, and Lutz Jancke. Electrical brain imaging reveals spatio-temporal dynamics of timbre perception in humans. *Neuroimage*, 32(4):1510–1523, 2006.
- [116] Eleni Miliotou, Panagiotis Kyriakis, Jason D Hinman, Andrei Irimia, and Paul Bogdan. Generative decoding of visual stimuli. In Andreas Krause, Emma Brunskill, Kyunghyun Cho, Barbara Engelhardt, Sivan Sabato, and Jonathan Scarlett, editors, *Proceedings of the 40th International Conference on Machine Learning*, volume 202 of *Proceedings of Machine Learning Research*, pages 24775–24784. PMLR, 23–29 Jul 2023.
- [117] Rahul Mishra, Krishan Sharma, RR Jha, and Arnav Bhavsar. Neurogan: image reconstruction from eeg signals via an attention-based gan. *Neural Computing and Applications*, 35(12):9181–9192, 2023.
- [118] Yoichi Miyawaki, Hajime Uchida, Okito Yamashita, Masaki Sato, Yusuke Morito, Hiroki C Tanabe, Norihiro Sadato, and Yukiyasu Kamitani. Visual image reconstruction from human brain activity using a combination of multiscale local image decoders. *Neuron*, 60(5):915–929, 2008.
- [119] Patricia Morosan, Jorg Rademacher, Axel Schleicher, Katrin Amunts, Thorsten Schormann, and Karl Zilles. Human primary auditory cortex: cytoarchitectonic subdivisions and mapping into a spatial reference system. *Neuroimage*, 13(4):684–701, 2001.
- [120] Milad Mozafari, Leila Reddy, and Rufin VanRullen. Reconstructing natural scenes from fmri patterns using bigbigan. In *2020 International joint conference on neural networks (IJCNN)*, pages 1–8. IEEE, 2020.
- [121] Gernot R Müller-Putz, Reinhold Scherer, Gert Pfurtscheller, and Rüdiger Rupp. Eeg-based neuroprosthesis control: a step towards clinical practice. *Neuroscience letters*, 382(1-2):169–174, 2005.
- [122] Mariacristina Musso, Andrea Moro, Volkmar Glauche, Michel Rijntjes, Jürgen Reichenbach, Christian Büchel, and Cornelius Weiller. Broca’s area and the language instinct. *Nature neuroscience*, 6(7):774–781, 2003.
- [123] Tomoya Nakai, Naoko Koide-Majima, and Shinji Nishimoto. Music genre neuroimaging dataset. *Data in Brief*, 40:107675, 2022.
- [124] Samuel A Nastase, Yun-Fei Liu, Hanna Hillman, Asieh Zadbood, Liat Hasenfratz, Neggin Keshavarzian, Janice Chen, Christopher J Honey, Yaara Yeshurun, Mor Regev, et al. The “narratives” fmri dataset for evaluating models of naturalistic language comprehension. *Scientific data*, 8(1):250, 2021.
- [125] Anh Nguyen, Alexey Dosovitskiy, Jason Yosinski, Thomas Brox, and Jeff Clune. Synthesizing the preferred inputs for neurons in neural networks via deep generator networks. *Advances in neural information processing systems*, 29, 2016.
- [126] Shinji Nishimoto, An T Vu, Thomas Naselaris, Yuval Benjamin, Bin Yu, and Jack L Gallant. Reconstructing visual experiences from brain activity evoked by natural movies. *Current biology*, 21(19):1641–1646, 2011.
- [127] Mizuho Nishio, Chihiro Nagashima, Saori Hirabayashi, Akinori Ohnishi, Kaori Sasaki, Tomoyuki Sagawa, Masayuki Hamada, and Tatsuo Yamashita. Convolutional auto-encoder for image denoising of ultra-low-dose ct. *Heliyon*, 3(8), 2017.
- [128] Aaron van den Oord, Sander Dieleman, Heiga Zen, Karen Simonyan, Oriol Vinyals, Alex Graves, Nal Kalchbrenner, Andrew Senior, and Koray Kavukcuoglu. Wavenet:

- A generative model for raw audio. *arXiv preprint arXiv:1609.03499*, 2016.
- [129] Furkan Ozcelik, Bhavin Choksi, Milad Mozafari, Leila Reddy, and Rufin VanRullen. Reconstruction of perceived images from fmri patterns and semantic brain exploration using instance-conditioned gans. In *2022 International Joint Conference on Neural Networks (IJCNN)*, pages 1–8. IEEE, 2022.
- [130] Furkan Ozcelik and Rufin VanRullen. Natural scene reconstruction from fmri signals using generative latent diffusion. *Scientific Reports*, 13(1):15666, 2023.
- [131] Simone Palazzo, Concetto Spampinato, Isaak Kavasidis, Daniela Giordano, Joseph Schmidt, and Mubarak Shah. Decoding brain representations by multimodal learning of neural activity and visual features. *IEEE Transactions on Pattern Analysis and Machine Intelligence*, 43(11):3833–3849, 2020.
- [132] Simone Palazzo, Concetto Spampinato, Isaak Kavasidis, Daniela Giordano, and Mubarak Shah. Generative adversarial networks conditioned by brain signals. In *Proceedings of the IEEE international conference on computer vision*, pages 3410–3418, 2017.
- [133] Kishore Papineni, Salim Roukos, Todd Ward, and Wei-Jing Zhu. Bleu: a method for automatic evaluation of machine translation. In *Proceedings of the 40th Annual Meeting on Association for Computational Linguistics*, pages 311–318, 2002.
- [134] Jong-Yun Park, Mitsuaki Tsukamoto, Misato Tanaka, and Yukiyasu Kamitani. Sound reconstruction from human brain activity via a generative model with brain-like auditory features. *arXiv preprint arXiv:2306.11629*, 2023.
- [135] Jonathan D Power, Damien A Fair, Bradley L Schlaggar, and Steven E Petersen. The development of human functional brain networks. *Neuron*, 67(5):735–748, 2010.
- [136] Xuelin Qian, Yikai Wang, Yanwei Fu, Xinwei Sun, Xiayang Xue, and Jianfeng Feng. Joint fmri decoding and encoding with latent embedding alignment, 2023.
- [137] Kai Qiao, Jian Chen, Linyuan Wang, Chi Zhang, Li Tong, and Bin Yan. Biggan-based bayesian reconstruction of natural images from human brain activity. *Neuroscience*, 444:92–105, 2020.
- [138] Alec Radford, Jong Wook Kim, Chris Hallacy, Aditya Ramesh, Gabriel Goh, Sandhini Agarwal, Girish Sastry, Amanda Askell, Pamela Mishkin, Jack Clark, et al. Learning transferable visual models from natural language supervision. In *International conference on machine learning*, pages 8748–8763. PMLR, 2021.
- [139] Alec Radford, Luke Metz, and Soumith Chintala. Unsupervised representation learning with deep convolutional generative adversarial networks. *arXiv preprint arXiv:1511.06434*, 2015.
- [140] Alec Radford, Karthik Narasimhan, Tim Salimans, Ilya Sutskever, et al. Improving language understanding by generative pre-training. 2018.
- [141] Alec Radford, Jeffrey Wu, Rewon Child, David Luan, Dario Amodei, Ilya Sutskever, et al. Language models are unsupervised multitask learners. *OpenAI blog*, 1(8):9, 2019.
- [142] Aravind Ravi, Jing Lu, Sarah Pearce, and Ning Jiang. Enhanced system robustness of asynchronous bci in augmented reality using steady-state motion visual evoked potential. *IEEE Transactions on Neural Systems and Rehabilitation Engineering*, 30:85–95, 2022.
- [143] Ali Razavi, Aaron Van den Oord, and Oriol Vinyals. Generating diverse high-fidelity images with vq-vae-2. *Advances in neural information processing systems*, 32, 2019.
- [144] Nils Reimers and Iryna Gurevych. Sentence-bert: Sentence embeddings using siamese bert-networks. In *Proceedings of the 2019 Conference on Empirical Methods in Natural Language Processing and the 9th International Joint Conference on Natural Language Processing (EMNLP-IJCNLP)*, pages 3982–3992, 2019.
- [145] Ziqi Ren, Jie Li, Xuotong Xue, Xin Li, Fan Yang, Zhicheng Jiao, and Xinbo Gao. Reconstructing seen image from brain activity by visually-guided cognitive representation and adversarial learning. *NeuroImage*, 228:117602, 2021.
- [146] Robin Rombach, Andreas Blattmann, Dominik Lorenz, Patrick Esser, and Björn Ommer. High-resolution image synthesis with latent diffusion models. In *Proceedings of the IEEE/CVF conference on computer vision and pattern recognition*, pages 10684–10695, 2022.
- [147] Olaf Ronneberger, Philipp Fischer, and Thomas Brox. U-net: Convolutional networks for biomedical image segmentation. In *Medical Image Computing and Computer-Assisted Intervention—MICCAI 2015: 18th International Conference, Munich, Germany, October 5-9, 2015, Proceedings, Part III 18*, pages 234–241. Springer, 2015.
- [148] Chitwan Saharia, William Chan, Saurabh Saxena, Lala Li, Jay Whang, Emily L Denton, Kamyar Ghasemipour, Raphael Gontijo Lopes, Burcu Karagol Ayan, Tim Salimans, et al. Photorealistic text-to-image diffusion models with deep language understanding. *Advances in Neural Information Processing Systems*, 35:36479–36494, 2022.
- [149] Masaki Saito, Eiichi Matsumoto, and Shunta Saito. Temporal generative adversarial nets with singular value clipping. In *Proceedings of the IEEE international conference on computer vision*, pages 2830–2839, 2017.
- [150] Sanne Schoenmakers, Markus Barth, Tom Heskes, and Marcel Van Gerven. Linear reconstruction of perceived images from human brain activity. *NeuroImage*, 83:951–961, 2013.
- [151] Paul S Scotti, Atmadeep Banerjee, Jimmie Goode, Stepan Shabalin, Alex Nguyen, Ethan Cohen, Aidan J Dempster, Nathalie Verlinde, Elad Yundler, David Weisberg, et al. Reconstructing the mind’s eye: fmri-to-image with contrastive learning and diffusion priors. *arXiv preprint arXiv:2305.18274*, 2023.
- [152] Katja Seeliger, Umut Güçlü, Luca Ambrogioni, Yagmur Güçlütürk, and Marcel AJ van Gerven. Generative adversarial networks for reconstructing natural images from brain activity. *NeuroImage*, 181:775–785, 2018.
- [153] Katja Seeliger, RP Sommers, U Güçlü, SE Bosch, and MAJ Van Gerven. A large single-participant fmri dataset for probing brain responses to naturalistic stimuli in space and time. *BioRxiv*, page 687681, 2019.

- [154] Guohua Shen, Kshitij Dwivedi, Kei Majima, Tomoyasu Horikawa, and Yukiyasu Kamitani. End-to-end deep image reconstruction from human brain activity. *Frontiers in computational neuroscience*, 13:21, 2019.
- [155] Guohua Shen, Tomoyasu Horikawa, Kei Majima, and Yukiyasu Kamitani. Deep image reconstruction from human brain activity. *PLoS computational biology*, 15(1):e1006633, 2019.
- [156] Karen Simonyan and Andrew Zisserman. Very deep convolutional networks for large-scale image recognition. *arXiv preprint arXiv:1409.1556*, 2014.
- [157] Prajwal Singh, Pankaj Pandey, Krishna Miyapuram, and Shanmuganathan Raman. Eeg2image: Image reconstruction from eeg brain signals. In *ICASSP 2023-2023 IEEE International Conference on Acoustics, Speech and Signal Processing (ICASSP)*, pages 1–5. IEEE, 2023.
- [158] Jascha Sohl-Dickstein, Eric Weiss, Niru Maheswaranathan, and Surya Ganguli. Deep unsupervised learning using nonequilibrium thermodynamics. In *International conference on machine learning*, pages 2256–2265. PMLR, 2015.
- [159] Kihyuk Sohn, Honglak Lee, and Xinchen Yan. Learning structured output representation using deep conditional generative models. *Advances in neural information processing systems*, 28, 2015.
- [160] Yang Song and Stefano Ermon. Generative modeling by estimating gradients of the data distribution. *Advances in neural information processing systems*, 32, 2019.
- [161] Yang Song, Jascha Sohl-Dickstein, Diederik P Kingma, Abhishek Kumar, Stefano Ermon, and Ben Poole. Score-based generative modeling through stochastic differential equations. *arXiv preprint arXiv:2011.13456*, 2020.
- [162] Concetto Spampinato, Simone Palazzo, Isaak Kavasidis, Daniela Giordano, Nasim Souly, and Mubarak Shah. Deep learning human mind for automated visual classification. In *Proceedings of the IEEE conference on computer vision and pattern recognition*, pages 6809–6817, 2017.
- [163] Jingyuan Sun, Mingxiao Li, Zijiao Chen, Yunhao Zhang, Shaonan Wang, and Marie-Francine Moens. Contrast, attend and diffuse to decode high-resolution images from brain activities. *arXiv preprint arXiv:2305.17214*, 2023.
- [164] Christian Szegedy, Vincent Vanhoucke, Sergey Ioffe, Jon Shlens, and Zbigniew Wojna. Rethinking the inception architecture for computer vision. In *Proceedings of the IEEE conference on computer vision and pattern recognition*, pages 2818–2826, 2016.
- [165] Saya Takada, Ren Togo, Takahiro Ogawa, and Miki Haseyama. Generation of viewed image captions from human brain activity via unsupervised text latent space. In *2020 IEEE International Conference on Image Processing (ICIP)*, pages 2521–2525. IEEE, 2020.
- [166] Yu Takagi and Shinji Nishimoto. High-resolution image reconstruction with latent diffusion models from human brain activity. In *Proceedings of the IEEE/CVF Conference on Computer Vision and Pattern Recognition*, pages 14453–14463, 2023.
- [167] Yu Takagi and Shinji Nishimoto. Improving visual image reconstruction from human brain activity using latent diffusion models via multiple decoded inputs. *arXiv preprint arXiv:2306.11536*, 2023.
- [168] Mingxing Tan and Quoc Le. Efficientnet: Rethinking model scaling for convolutional neural networks. In *International conference on machine learning*, pages 6105–6114. PMLR, 2019.
- [169] Jerry Tang, Meng Du, Vy A Vo, Vasudev Lal, and Alexander Huth. Brain encoding models based on multimodal transformers can transfer across language and vision. In *Thirty-seventh Conference on Neural Information Processing Systems*, 2023.
- [170] Jerry Tang, Amanda LeBel, Shailee Jain, and Alexander G Huth. Semantic reconstruction of continuous language from non-invasive brain recordings. *Nature Neuroscience*, pages 1–9, 2023.
- [171] Praveen Tirupattur, Yogesh Singh Rawat, Concetto Spampinato, and Mubarak Shah. Thoughtviz: Visualizing human thoughts using generative adversarial network. In *Proceedings of the 26th ACM international conference on Multimedia*, pages 950–958, 2018.
- [172] Frank Tong. Primary visual cortex and visual awareness. *Nature Reviews Neuroscience*, 4(3):219–229, 2003.
- [173] Pascale Tremblay and Steven L Small. On the context-dependent nature of the contribution of the ventral premotor cortex to speech perception. *NeuroImage*, 57(4):1561–1571, 2011.
- [174] Sergey Tulyakov, Ming-Yu Liu, Xiaodong Yang, and Jan Kautz. Mocogan: Decomposing motion and content for video generation. In *Proceedings of the IEEE conference on computer vision and pattern recognition*, pages 1526–1535, 2018.
- [175] Jagpal Singh Ubhi, Ashwani Kumar Aggarwal, et al. Neural style transfer for image within images and conditional gans for destylization. *Journal of Visual Communication and Image Representation*, 85:103483, 2022.
- [176] Aaron Van den Oord, Nal Kalchbrenner, Lasse Espeholt, Oriol Vinyals, Alex Graves, et al. Conditional image generation with pixelcnn decoders. *Advances in neural information processing systems*, 29, 2016.
- [177] Aaron Van Den Oord, Nal Kalchbrenner, and Koray Kavukcuoglu. Pixel recurrent neural networks. In *International conference on machine learning*, pages 1747–1756. PMLR, 2016.
- [178] Aaron Van Den Oord, Oriol Vinyals, et al. Neural discrete representation learning. *Advances in neural information processing systems*, 30, 2017.
- [179] David C Van Essen, Stephen M Smith, Deanna M Barch, Timothy EJ Behrens, Essa Yacoub, Kamil Ugurbil, Wu-Minn HCP Consortium, et al. The wu-minn human connectome project: an overview. *Neuroimage*, 80:62–79, 2013.
- [180] Marcel AJ Van Gerven, Floris P De Lange, and Tom Heskes. Neural decoding with hierarchical generative models. *Neural computation*, 22(12):3127–3142, 2010.
- [181] Rufin VanRullen and Leila Reddy. Reconstructing faces from fmri patterns using deep generative neural networks. *Communications biology*, 2(1):193, 2019.

- [182] Ashish Vaswani, Noam Shazeer, Niki Parmar, Jakob Uszkoreit, Llion Jones, Aidan N Gomez, Łukasz Kaiser, and Illia Polosukhin. Attention is all you need. *Advances in neural information processing systems*, 30, 2017.
- [183] Chong Wang, Hongmei Yan, Wei Huang, Jiyi Li, Yuting Wang, Yun-Shuang Fan, Wei Sheng, Tao Liu, Rong Li, and Huaifu Chen. Reconstructing rapid natural vision with fmri-conditional video generative adversarial network. *Cerebral Cortex*, 32(20):4502–4511, 2022.
- [184] Jianfeng Wang, Zhengyuan Yang, Xiaowei Hu, Linjie Li, Kevin Lin, Zhe Gan, Zicheng Liu, Ce Liu, and Lijuan Wang. Git: A generative image-to-text transformer for vision and language. *arXiv preprint arXiv:2205.14100*, 2022.
- [185] Ting-Chun Wang, Ming-Yu Liu, Jun-Yan Zhu, Guilin Liu, Andrew Tao, Jan Kautz, and Bryan Catanzaro. Video-to-video synthesis. *arXiv preprint arXiv:1808.06601*, 2018.
- [186] Zhou Wang, Alan C Bovik, Hamid R Sheikh, and Eero P Simoncelli. Image quality assessment: from error visibility to structural similarity. *IEEE transactions on image processing*, 13(4):600–612, 2004.
- [187] Dong Wen, Bingbing Liang, Yanhong Zhou, Hongqian Chen, and Tzyy-Ping Jung. The current research of combining multi-modal brain-computer interfaces with virtual reality. *IEEE Journal of Biomedical and Health Informatics*, 25(9):3278–3287, 2020.
- [188] Haiguang Wen, Junxing Shi, Yizhen Zhang, Kun-Han Lu, Jiayue Cao, and Zhongming Liu. Neural encoding and decoding with deep learning for dynamic natural vision. *Cerebral cortex*, 28(12):4136–4160, 2018.
- [189] Chenfei Wu, Jian Liang, Lei Ji, Fan Yang, Yuejian Fang, Daxin Jiang, and Nan Duan. Nüwa: Visual synthesis pre-training for neural visual world creation. In *European conference on computer vision*, pages 720–736. Springer, 2022.
- [190] Nuwa Xi, Sendong Zhao, Haochun Wang, Chi Liu, Bing Qin, and Ting Liu. Unicorn: Unified cognitive signal reconstruction bridging cognitive signals and human language. *arXiv preprint arXiv:2307.05355*, 2023.
- [191] Weihao Xia, Raoul de Charette, Cengiz Öztireli, and Jing-Hao Xue. Dream: Visual decoding from reversing human visual system. *arXiv preprint arXiv:2310.02265*, 2023.
- [192] Jianxiong Xiao, James Hays, Krista A Ehinger, Aude Oliva, and Antonio Torralba. Sun database: Large-scale scene recognition from abbey to zoo. In *2010 IEEE computer society conference on computer vision and pattern recognition*, pages 3485–3492. IEEE, 2010.
- [193] Xingqian Xu, Zhangyang Wang, Eric Zhang, Kai Wang, and Humphrey Shi. Versatile diffusion: Text, images and variations all in one diffusion model. *arXiv preprint arXiv:2211.08332*, 2022.
- [194] Zesheng Ye, Lina Yao, Yu Zhang, and Sylvia Gustin. Self-supervised cross-modal visual retrieval from brain activities. *Pattern Recognition*, 145:109915, 2024.
- [195] Jaechang Yoo, Heesong Eom, and Yong Suk Choi. Image-to-image translation using a cross-domain auto-encoder and decoder. *Applied Sciences*, 9(22):4780, 2019.
- [196] Neil Zeghidour, Alejandro Luebs, Ahmed Omran, Jan Skoglund, and Marco Tagliasacchi. Soundstream: An end-to-end neural audio codec. *IEEE/ACM Transactions on Audio, Speech, and Language Processing*, 30:495–507, 2021.
- [197] Neil Zeghidour, Olivier Teboul, Félix de Chaumont Quitry, and Marco Tagliasacchi. Leaf: A learnable frontend for audio classification. *arXiv preprint arXiv:2101.08596*, 2021.
- [198] Bohan Zeng, Shanglin Li, Xuhui Liu, Sicheng Gao, Xiaolong Jiang, Xu Tang, Yao Hu, Jianzhuang Liu, and Baochang Zhang. Controllable mind visual diffusion model. *arXiv preprint arXiv:2305.10135*, 2023.
- [199] Hong Zeng, Nianzhang Xia, Dongguan Qian, Motonobu Hattori, Chu Wang, and Wanzeng Kong. Dm-re2i: A framework based on diffusion model for the reconstruction from eeg to image. *Biomedical Signal Processing and Control*, 86:105125, 2023.
- [200] Jiang Zhang, Chen Li, Ganwanming Liu, Min Min, Chong Wang, Jiyi Li, Yuting Wang, Hongmei Yan, Zhentao Zuo, Wei Huang, et al. A cnn-transformer hybrid approach for decoding visual neural activity into text. *Computer Methods and Programs in Biomedicine*, 214:106586, 2022.
- [201] Lvmin Zhang, Anyi Rao, and Maneesh Agrawala. Adding conditional control to text-to-image diffusion models. In *Proceedings of the IEEE/CVF International Conference on Computer Vision*, pages 3836–3847, 2023.
- [202] Tianyi Zhang, Varsha Kishore, Felix Wu, Kilian Q Weinberger, and Yoav Artzi. Bertscore: Evaluating text generation with bert. In *International Conference on Learning Representations*, 2019.
- [203] Yifei Zhang. A better autoencoder for image: Convolutional autoencoder. In *ICONIP17-DCEC. Available online: http://users.cecs.anu.edu.au/Tom.Gedeon/conf/ABCs2018/paper/ABCs2018_paper_58.pdf (accessed on 23 March 2017)*, 2018.
- [204] Jun-Yan Zhu, Taesung Park, Phillip Isola, and Alexei A Efros. Unpaired image-to-image translation using cycle-consistent adversarial networks. In *Proceedings of the IEEE international conference on computer vision*, pages 2223–2232, 2017.